


Thermodynamic uncertainty relation for energy transport in a transient regime: A model study

Sushant Saryal, Onkar Sadekar , and Bijay Kumar Agarwalla ^{*}

Department of Physics, Indian Institute of Science Education and Research, Pune 411008, India

 (Received 25 August 2020; revised 5 January 2021; accepted 3 February 2021; published 26 February 2021)

We investigate a transient version of the recently discovered thermodynamic uncertainty relation (TUR) which provides a precision-cost trade-off relation for certain out-of-equilibrium thermodynamic observables in terms of net entropy production. We explore this relation in the context of energy transport in a bipartite setting for three exactly solvable toy model systems (two coupled harmonic oscillators, two coupled qubits, and a hybrid coupled oscillator-qubit system) and analyze the role played by the underlying statistics of the transport carriers in the TUR. Interestingly, for all these models, depending on the statistics, the TUR ratio can be expressed as a sum or a difference of a universal term which is always greater than or equal to 2 and a corresponding entropy production term. We find that the generalized version of the TUR, originating from the universal fluctuation symmetry, is always satisfied. However, interestingly, the specialized TUR, a tighter bound, is always satisfied for the coupled harmonic oscillator system obeying Bose-Einstein statistics. Whereas, for both the coupled qubit, obeying Fermi-like statistics, and the hybrid qubit-oscillator system with mixed Fermi-Bose statistics, violation of the tighter bound is observed in certain parameter regimes. We have provided conditions for such violations. We also provide a rigorous proof following the nonequilibrium Green's function approach that the tighter bound is always satisfied in the weak-coupling regime for generic bipartite systems.

DOI: [10.1103/PhysRevE.103.022141](https://doi.org/10.1103/PhysRevE.103.022141)

I. INTRODUCTION

Small scale systems are prone to fluctuations [1]. Characterizing and quantifying thermal and quantum fluctuations for small scale systems are therefore important both from the fundamental and as well as practical points of view [2,3]. The last two decades have seen a plethora of interesting works in this direction. In particular, the discovery of nonequilibrium universal fluctuation relations [4–14], concerning the microscopic description of systems, have provided a deeper understanding about nonequilibrium thermodynamics and have greatly contributed in establishing the rapidly growing field of stochastic and quantum thermodynamics [15–18].

Along this direction, very recently an interesting trade-off relation involving relative fluctuations of certain nonequilibrium observables has been put forward, providing a lower bound on these fluctuations in terms of the associated entropy production. Various versions of this relation, now collectively referred to as the thermodynamic uncertainty relations (TURs), have been proposed and furthermore its generality has been examined in many different contexts, such as for steady-state systems following classical Markovian dynamics, periodically driven systems, quantum transport problems, molecular motors, finite-time statistics, first-passage times, etc. [19–68]. Parallel to these theoretical developments, experimental studies of TURs for classical and quantum systems have also been reported very recently [68–71].

Here we are interested in understanding the transient version of the TUR in the context of energy exchange

that takes place between two quantum systems which are initially equilibrated at different temperatures. For such transport, a nonuniversal tighter version of the TUR bound (T-TUR) [19–22], is given as (we set $k_B = 1$)

$$\frac{\langle Q^2 \rangle_c}{\langle Q \rangle^2} \geq \frac{2}{\langle \Sigma \rangle}, \quad (1)$$

where Q , a stochastic variable, is the integrated energy current over a certain time duration. $\langle Q \rangle$ and $\langle Q^2 \rangle_c$ represent the average energy exchange and the corresponding noise, respectively. $\langle \Sigma \rangle \geq 0$ represents the average entropy production in the energy exchange process and further characterizes how far the composite system is driven away from the initial condition. This bound was first put forward for steady-state systems driven by multiple affinities [19] in the linear response regime and later a rigorous proof was given for systems following continuous-time Markov jump processes [20].

A loose but a generalized version of the bound (G-TUR1) compared to Eq. (1) [42] was recently derived following the fundamental energy exchange fluctuation theorem (XFT) relation [9], where the right-hand side of Eq. (1) was modified to

$$\frac{\langle Q^2 \rangle_c}{\langle Q \rangle^2} \geq \frac{2}{\exp \langle \Sigma \rangle - 1}. \quad (2)$$

In fact, a tighter version [still loose compared to Eq. (1)] of the generalized bound in Eq. (2) was obtained by Timpanaro *et al.* [56] (G-TUR2), given as

$$\frac{\langle Q^2 \rangle_c}{\langle Q \rangle^2} \geq f(\langle \Sigma \rangle), \quad (3)$$

^{*}bijay@iiserpune.ac.in

where $f(x) = \text{csch}^2(g(x/2))$ and $g(x)$ is the inverse function of $x \tanh(x)$.

Of course, it is clear that systems satisfying the XFT will follow the G-TUR1 and G-TUR2. However, it is still an interesting question to ask under what conditions the tighter version, i.e., the T-TUR bound in Eq. (1), will be preserved. Very recently, the usefulness of the T-TUR bound was proposed to infer the net entropy production for complex nonequilibrium systems [72].

In this work, we analyze TUR bounds for quantum energy transport by focusing on three different model systems characterized by different quantum statistics: bosonic, fermionic, and hybrid Fermi-Bose statistics for the transport carriers. Since it is well known that quantum statistics plays a key role in the transport properties, we ask, how does it affect the transient TUR bounds? Interestingly, we find that when energy exchange takes place between two simple quantum harmonic oscillators, obeying Bose-Einstein statistics, the T-TUR in Eq. (1) is always satisfied, whereas in the other extreme scenario, i.e., when each system consists of a single qubit, following Fermi-like statistics, violation for the T-TUR is observed in certain parameter regimes. As a final interesting example, we consider a hybrid setup consisting of a single quantum harmonic oscillator and a qubit and analyze the impact of hybrid statistics on the TUR. We also show that for a general bipartite setup, the T-TUR is always satisfied in the weak-coupling regime. Expectedly, in all these setups, the generalized version of TUR is satisfied due to the underlying XFT for energy exchange.

The paper is organized as follows: We start in Sec. II with a brief introduction about obtaining the characteristic function (CF) for the energy exchange following the two-time measurement protocol and describe the associated XFT. In Sec. III we introduce three toy models, provide derivation for the exact CFs, and analyze the corresponding TUR. In Sec. IV we provide a proof for the T-TUR in the weak-coupling regime in both transient and steady-state limits. We summarize our main findings in Sec. V. We delegate certain details to the Appendixes.

II. ENERGY EXCHANGE STATISTICS AND THE CHARACTERISTIC FUNCTION

In this section we briefly outline the theory behind obtaining the quantum energy exchange statistics for a generic out-of-equilibrium bipartite setup. Under this setting, one considers two systems with Hamiltonians H_1 and H_2 that are initially ($t = 0^-$) decoupled with composite density matrix given by a product state, $\rho(0) = \rho_1 \otimes \rho_2$, with $\rho_i = \exp[-\beta_i H_i] / \mathcal{Z}_i$, $i = 1, 2$, being the initial Gibbs thermal state with inverse temperature $\beta_i = 1/T_i$ (we set $k_B = \hbar = 1$) and $\mathcal{Z}_i = \text{Tr}[e^{-\beta_i H_i}]$ is the corresponding canonical partition function. To allow energy exchange, an interaction term between the two systems, denoted as V , is suddenly switched on at $t = 0$ and suddenly switched off after a duration of $t = T$. The composite system in this interval evolves unitarily with the total Hamiltonian $H = H_1 + H_2 + V$.

It is now a well known fact that for quantum systems quantities such as integrated energy current, work, or the associated entropy production are not direct observables but

rather depend on the measurements of relevant Hamiltonians at the initial and final times of the process. Therefore, to construct the probability distribution function (PDF) [10,11,14] for energy exchange, projective measurements of the system Hamiltonians H_1 and H_2 should be carried out simultaneously in the beginning and at the end of the process. Following this, the joint PDF, $p_T(\Delta E_1, \Delta E_2)$, corresponding to the energy change (ΔE_i , $i = 1, 2$) of both the systems can be constructed as

$$p_T(\Delta E_1, \Delta E_2) = \sum_{m,n} \left(\prod_{i=1}^2 \delta(\Delta E_i - (\epsilon_m^i - \epsilon_n^i)) \right) p_{m|n}^T p_n^0, \quad (4)$$

where $p_n^0 = \prod_{i=1}^2 e^{-\beta_i \epsilon_n^i} / \mathcal{Z}_i$ corresponds to the probability to find the system initially in the common energy eigenstate $|n\rangle = |n_1, n_2\rangle$ of the composite system where $|n_i\rangle$ and ϵ_n^i are energy eigenstate and eigenvalue, respectively, of system i after the first projective measurement. The second projective measurement at the final time ($t = T$) leads to the collapse of the state of the composite system to another common energy eigenstate $|m\rangle = |m_1, m_2\rangle$. The transition probability between these states is given by $p_{m|n}^T = |\langle m | \mathcal{U}(T, 0) | n \rangle|^2$ with $\mathcal{U}(t, 0) = e^{-iHt}$ being the global unitary propagator with the total Hamiltonian H . Now one can show that for autonomous and time-reversal invariant quantum systems evolving unitarily $p_{m|n}^T = p_{n|m}^T$. This condition is also known as the principle of microreversibility in the literature [10,11]. Using this condition in Eq. (4) one receives the following universal symmetry for this joint PDF:

$$p_T(\Delta E_1, \Delta E_2) = e^{\beta_1 \Delta E_1 + \beta_2 \Delta E_2} p_T(-\Delta E_1, -\Delta E_2). \quad (5)$$

At this junction, it is important to point out that under the general coupling scenario the energy change of an individual system cannot be interpreted as heat, as a part of the energy change may be used in turning on and off the interaction (V) between the two systems. However, in the weak-coupling limit ($V \ll H_{1,2}$), it is safe to interpret this energy change as heat. One can then define heat as $Q = -\Delta E_1 \approx \Delta E_2$ which following Eq. (5) then leads to a heat exchange fluctuation relation (XFT)

$$p_T(Q) = e^{\Delta\beta Q} p_T(-Q), \quad (6)$$

where $\Delta\beta = \beta_2 - \beta_1$. As per our convention, heat flowing out from system 1 to system 2 is considered positive.

The central object of interest in our work is the CF corresponding to the PDF for energy exchange which is obtained by performing a Fourier transformation (FT) of the probability distribution:

$$\begin{aligned} \chi_T(u) &= \int dQ e^{iuQ} p_T(Q) \\ &= \text{Tr}[\mathcal{U}^\dagger(T, 0)(e^{-iuH_1} \otimes 1_2)\mathcal{U}(T, 0)(e^{iuH_1} \otimes 1_2)\rho(0)]. \end{aligned} \quad (7)$$

Here u is a variable conjugate to Q . In terms of CF, the XFT for heat in Eq. (6) translates to $\chi_T(u) = \chi_T(-u + i\Delta\beta)$ [9,73–77].

It is important to note that, for a special choice of the coupling Hamiltonian V , satisfying the commutation relation

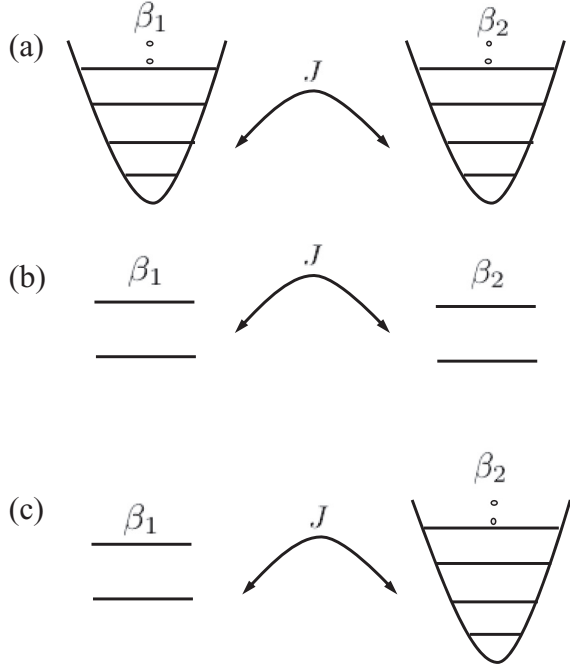


FIG. 1. Schematic for three different toy models that we investigate in this paper: (a) the coupled two-oscillator system, (b) the coupled two-qubit system, and (c) the coupled hybrid qubit-oscillator system. Each system is prepared initially in equilibrium at a particular inverse temperature $\beta_i = 1/k_B T_i$. A finite thermal coupling with coupling strength J allows energy exchange between the systems.

$[V, H_1 + H_2] = 0$, the total internal energy $H_1 + H_2$ is a constant of motion which implies that the change of energy for one system is exactly compensated by the other one. In other words, there is no energy cost involved in turning on and off the interaction between the systems. Such a type of coupling is known as the thermal coupling. Therefore, under this symmetry condition the definition for heat, $Q = -\Delta E_1 = \Delta E_2$, becomes exact for arbitrary coupling strength. More generally, the XFT for heat is preserved exactly in this limit (see Appendix A for the details of the proof following the CF of heat).

In what follows, we study three different toy models with different underlying quantum statistics in the thermal coupling limit, thus getting rid of any ambiguity with the definition for heat. We derive exact analytical expressions for the CF and then analyze the impact of quantum statistics on the TUR bounds.

III. MODELS AND TUR

A. Two-oscillator system

As a first example, we consider a bipartite setup where each system consists of a single quantum harmonic oscillator [see Fig. 1(a)]. The total Hamiltonian is given as

$$H_{\text{osc}} = \omega_0 a_1^\dagger a_1 \otimes \mathbb{1}_2 + \mathbb{1}_1 \otimes \omega_0 a_2^\dagger a_2 + J (a_1^\dagger \otimes a_2 + a_2^\dagger \otimes a_1), \quad (8)$$

where the first two terms ($H_1 = \omega_0 a_1^\dagger a_1 \otimes \mathbb{1}_2$ and $H_2 = \mathbb{1}_1 \otimes \omega_0 a_2^\dagger a_2$) correspond to two noninteracting quantum harmonic

oscillators with a_i (a_i^\dagger) being the bosonic annihilation (creation) operator for the i th oscillator. The last term, denoted here as V , represents a bilinear interaction between the oscillators with coupling strength J . Note that the frequency of both the oscillators (ω_0) is chosen to be identical which ensures the thermal coupling condition, i.e., $[V, H_1 + H_2] = 0$. Recall that, before turning on the interaction V , each oscillator is thermalized independently at a particular temperature which can be achieved by placing the system in weak contact with a thermal bath. After that, the oscillators are separated from the bath and the interaction between them is turned on to allow energy exchange for a certain duration T . The corresponding cumulant generating function (CGF) $\mathcal{G}_T^{\text{osc}}(u) = \ln \chi_T^{\text{osc}}(u)$ can be obtained exactly and is given as

$$\mathcal{G}_T^{\text{osc}}(u) = -\ln[1 - \sin^2(JT)\{n_1(\omega_0)(1 + n_2(\omega_0))(e^{iu\omega_0} - 1) + n_2(\omega_0)(1 + n_1(\omega_0))(e^{-iu\omega_0} - 1)\}], \quad (9)$$

where $n_i(\omega_0) = (e^{\beta_i \omega_0} - 1)^{-1}$, $i = 1, 2$, is the Bose-Einstein distribution function. We provide the derivation of Eq. (9) in Appendix C by employing the Keldysh nonequilibrium Green's function (NEGF) approach [78–82]. Note that a similar model was previously studied in the context of fluctuation symmetry where the CGF was obtained only in the weak-coupling regime [83]. Very recently, this model was studied in the context of quantum heat engines [62]. It is easy to verify that the above CGF expression preserves the XFT for arbitrary T , J , β_1 , and β_2 .

To analyze the TUR bound, we now get the expressions for the average energy change and the associated noise. These are easily obtained by taking successive derivatives of $\mathcal{G}_T^{\text{osc}}(u)$ with respect to iu . We receive, (for notational compactness, below we denote $n_i(\omega_0)$ as n_i)

$$\langle Q \rangle^{\text{osc}} = \omega_0 \mathcal{T}_T(J) [n_1 - n_2], \quad (10)$$

$$\langle Q^2 \rangle_c^{\text{osc}} = \omega_0^2 [\mathcal{T}_T(J) (n_1(1 + n_2) + n_2(1 + n_1)) + \mathcal{T}_T^2(J) (n_1 - n_2)^2], \quad (11)$$

where we define $\mathcal{T}_T(J) = \sin^2(JT)$. Since the second term in Eq. (11) is always positive, we receive the following inequality,

$$\langle Q^2 \rangle_c^{\text{osc}} \geq \omega_0^2 \mathcal{T}_T(J) (n_1(1 + n_2) + n_2(1 + n_1)), \quad (12)$$

where the equality sign corresponds to an equilibrium situation, i.e., $\beta_1 = \beta_2$. We now make use of the following important relation involving the Bose-Einstein distribution function,

$$n_1(1 + n_2) + n_2(1 + n_1) = \coth \frac{\Delta\beta\omega_0}{2} (n_1 - n_2) \quad (13)$$

$$\geq \frac{2}{\Delta\beta\omega_0} (n_1 - n_2), \quad (14)$$

where in the second line we have used the inequality $x \coth(x) \geq 1$. Substituting this in Eq. (12) and using Eq. (10), it is easy to see that $\Delta\beta \frac{\langle Q^2 \rangle_c^{\text{osc}}}{\langle Q \rangle^{\text{osc}}} \geq 2$, which implies that for the coupled quantum harmonic oscillator setup displaying bosonic statistics the T-TUR is always satisfied.

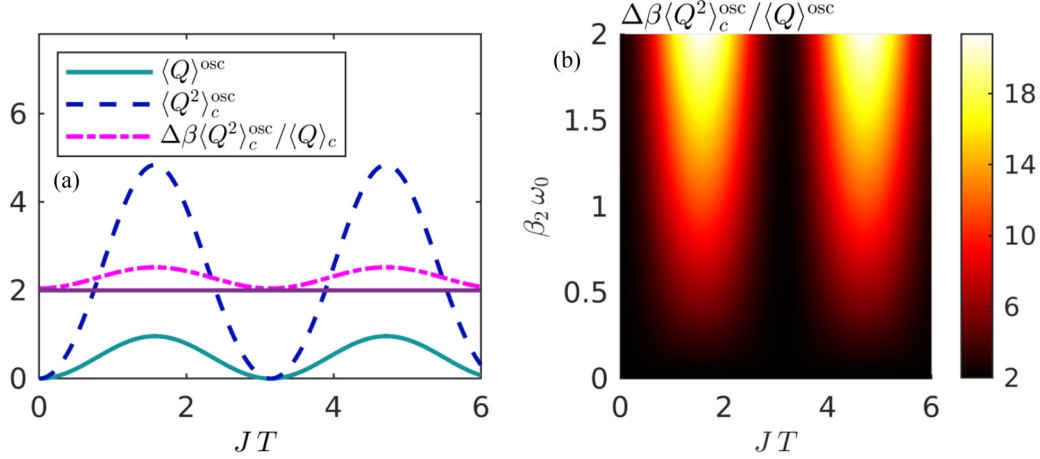


FIG. 2. (a) Plot for average energy change $\langle Q \rangle^{\text{osc}}$ (solid line), fluctuation $\langle Q^2 \rangle_c^{\text{osc}}$ (dashed line), and the corresponding TUR ratio $\Delta\beta \langle Q^2 \rangle_c^{\text{osc}} / \langle Q \rangle_c^{\text{osc}}$ (dash-dotted line) as a function of JT . For reference a line is drawn at the value 2. The parameters are $\beta_1 \omega_0 = 0.5$, $\beta_2 \omega_0 = 1$. (b) Two-dimensional plot for TUR ratio ($\Delta\beta \frac{\langle Q^2 \rangle_c^{\text{osc}}}{\langle Q \rangle_c^{\text{osc}}}$) as a function of JT and $\beta_2 \omega_0$. We set $\beta_1 \omega_0 = 0.1$.

In fact, an interesting observation can be made by arranging the TUR ratio ($\Delta\beta \frac{\langle Q^2 \rangle_c^{\text{osc}}}{\langle Q \rangle_c^{\text{osc}}}$) using the expressions for the cumulants [Eqs. (10) and (11)] and Eq. (13). One receives

$$\Delta\beta \frac{\langle Q^2 \rangle_c^{\text{osc}}}{\langle Q \rangle_c^{\text{osc}}} = \Delta\beta \omega_0 \coth \frac{\Delta\beta \omega_0}{2} + \langle \Sigma \rangle^{\text{osc}} \geq 2. \quad (15)$$

Interestingly, the first term here is independent of the coupling information between the systems and is always greater than or equal to 2 (equality holds in equilibrium). In contrast, the second term is exactly the average entropy production $\langle \Sigma \rangle^{\text{osc}} = \Delta\beta \langle Q \rangle^{\text{osc}}$ for the oscillator system which along with the temperature difference also importantly depends on the dimensionless coupling JT . As the average entropy production always remains positive, $\langle \Sigma \rangle^{\text{osc}} \geq 0$, once again we arrive at the same conclusion that the T-TUR for this setup is always satisfied. Also note that the validity of T-TUR immediately implies that the G-TUR1 [Eq. (2)] and G-TUR2 [Eq. (3)] are also trivially obeyed. Note that the meaning of entropy production should be understood here as the entropy that gets produced in the heat baths when we couple each subsystem with their respective heat baths after switching off the interaction V at the end of the energy exchange process at time T .

In Fig. 2(a) we plot the first two cumulants and the corresponding TUR ratio as a function of JT . Figure 2(b) corresponds to a two-dimensional plot for the TUR ratio as a function of JT and $\beta_2 \omega_0$. We set $\beta_1 \omega_0 = 0.1$ in the simulation. The cumulants as well as the TUR ratio oscillate with JT with periodicity π . The value for the TUR ratio is always larger than 2 and matches with the theoretical prediction. For a fixed value of JT , the TUR ratio increases monotonically with increasing $\Delta\beta$.

B. Two-qubit system

We next consider another toy model, which we refer here as the XY model, consisting of two qubits [see Fig. 1(b)]. We

write the total Hamiltonian as

$$H_{XY} = \frac{\omega_0}{2} \sigma_1^z \otimes \mathbb{1}_2 + \mathbb{1}_1 \otimes \frac{\omega_0}{2} \sigma_2^z + \frac{J}{2} (\sigma_1^x \otimes \sigma_2^y - \sigma_1^y \otimes \sigma_2^x), \quad (16)$$

where σ_i , $i = x, y, z$, are the standard Pauli matrices. Once again, this model satisfies the thermal coupling condition. Very recently, this model was experimentally realized by some of us in the nuclear magnetic resonance (NMR) setup to assess the validity of the transient TUR by obtaining the cumulants of energy exchange following the quantum state tomography technique [69]. The same model was also used earlier to examine the XFT by measuring the CF for heat exchange employing the ancilla-based interferometric technique [84–87]. We therefore keep some of our discussion here brief and request the readers to see Ref. [69] for the details about the model.

One can analytically compute the CGF of the energy exchange following Eq. (7) by performing simple algebraic manipulations of the Pauli matrices, which yields [87]

$$\mathcal{G}_T^{\text{spin}}(u) = \ln[1 + \sin^2(JT) \{f_1(\omega_0)(1 - f_2(\omega_0))(e^{iu\omega_0} - 1) + f_2(\omega_0)(1 - f_1(\omega_0))(e^{-iu\omega_0} - 1)\}], \quad (17)$$

where $f_i(\omega_0) = (e^{\beta_i \omega_0} + 1)^{-1}$, $i = 1, 2$, is the Fermi-like distribution function. Once again the XFT is obeyed for arbitrary J , T , β_1 , and β_2 due to the thermal coupling symmetry. At this point, it is important to compare the CGF in Eq. (17) with the CGF for the coupled oscillator in Eq. (9). First of all, for both these models, interestingly the JT dependence appears in the same functional form $\mathcal{T}_T(J) = \sin^2(JT)$. In fact, in this context it is simply the transition probability between states $|01\rangle$ and $|10\rangle$, i.e., $\mathcal{T}_T(J) = |\langle 10 | \mathcal{U}(T, 0) | 01 \rangle|^2$ [$|0\rangle$ ($|1\rangle$) refers to the ground (excited) state for the qubit]. Second and most importantly, there are crucial sign differences in terms of the Bose and Fermi-like functions, reflecting the key difference between a two-level spin system and an infinite-level harmonic oscillator system. In fact, because of this crucial sign change for the qubit setup, a looser bound for TUR appears,

as we show below. We once again write down the first two cumulants following the CGF as

$$\langle Q \rangle^{\text{spin}} = \omega_0 \mathcal{T}_T(J) [f_1 - f_2], \quad (18)$$

$$\langle Q^2 \rangle_c^{\text{spin}} = \omega_0^2 [\mathcal{T}_T(J) (f_1(1 - f_2) + f_2(1 - f_1)) - \mathcal{T}_T^2(J) (f_1 - f_2)^2]. \quad (19)$$

Interestingly, for a Fermi-like function also a relation similar to Eq. (13) exists, given as

$$f_1(1 - f_2) + f_2(1 - f_1) = \coth \frac{\Delta\beta\omega_0}{2} (f_1 - f_2). \quad (20)$$

This helps us to organize the cumulants and to receive the TUR ratio as

$$\Delta\beta \frac{\langle Q^2 \rangle_c^{\text{spin}}}{\langle Q \rangle^{\text{spin}}} = \Delta\beta\omega_0 \coth \left[\frac{\Delta\beta\omega_0}{2} \right] - \langle \Sigma \rangle^{\text{spin}}. \quad (21)$$

Once again this expression should be compared with Eq. (15). The first term is the same as before. However, the apparent sign differences between the two models reflect in the second term where the average entropy production term appears as a negative contribution to the TUR ratio. It is therefore not immediately obvious that this coupled two-qubit model will satisfy the T-TUR bound. In what follows we therefore first get an upper bound on the average entropy production and thereby provide a lower bound for the TUR. Interestingly, this helps us to find a condition on $\mathcal{T}_T(J)$ for which the T-TUR is respected.

We first note that the Fermi-like function can be alternatively written as

$$f_i = \frac{1}{e^{\beta_i\omega_0} + 1} = \frac{1}{2} \left(1 - \tanh \frac{\beta_i\omega_0}{2} \right). \quad (22)$$

With the help of this expression, we write down the net entropy production as

$$\begin{aligned} \langle \Sigma \rangle^{\text{spin}} &= \frac{\Delta\beta\omega_0 \mathcal{T}_T(J)}{2} \left[\tanh \frac{\beta_2\omega_0}{2} - \tanh \frac{\beta_1\omega_0}{2} \right] \\ &= \frac{\Delta\beta\omega_0 \mathcal{T}_T(J)}{2} \left[\left(\tanh \frac{\Delta\beta\omega_0}{2} \right) \right. \\ &\quad \left. \times \left(1 - \tanh \frac{\beta_1\omega_0}{2} \tanh \frac{\beta_2\omega_0}{2} \right) \right]. \end{aligned} \quad (23)$$

Now since β_i is always positive and $\tanh x$ is a bounded function between (0,1) for $x > 0$, the second term in the product in the above equation is always < 1 , which gives us

$$\tanh \frac{\Delta\beta\omega_0}{2} \geq \tanh \frac{\beta_2\omega_0}{2} - \tanh \frac{\beta_1\omega_0}{2}, \quad (24)$$

and therefore, we receive an upper bound for the average entropy production,

$$\langle \Sigma \rangle^{\text{spin}} \leq \frac{\Delta\beta\omega_0 \mathcal{T}_T(J)}{2} \tanh \frac{\Delta\beta\omega_0}{2}, \quad (25)$$

which finally translates to a lower bound on the TUR ratio for this model as

$$\Delta\beta \frac{\langle Q^2 \rangle_c^{\text{spin}}}{\langle Q \rangle^{\text{spin}}} \geq \Delta\beta\omega_0 \left[\coth \frac{\Delta\beta\omega_0}{2} - \frac{\mathcal{T}_T(J)}{2} \tanh \frac{\Delta\beta\omega_0}{2} \right]. \quad (26)$$

The equality sign here holds for $\beta_1 = 0$ or $\beta_2 = 0$ or $\Delta\beta = 0$. Since the TUR ratio is periodic as a function of JT , we focus our attention within the first period $[0, \pi]$. The obtained bound indicates that, in the weak-coupling limit, i.e., $JT \ll 1$ which implies $\mathcal{T}_T(J) \ll 1$, the second term in the above expression can be ignored and the T-TUR will be satisfied. In fact, it is easy to check that the T-TUR will remain valid for $\mathcal{T}_T(J) < 2/3$, which gives an allowed range for JT ($JT \leq 0.95$ and $JT \geq 2.19$, within the first period). Therefore, to observe a violation for the T-TUR, a necessary condition is to tune the value of JT such that $\mathcal{T}_T(J) > 2/3$. However, note that this condition is not a sufficient one. This can be seen as follows: following the right-hand side of Eq. (26), the minimum value for the TUR bound corresponds to $\mathcal{T}_T(J) = 1$. Now for large $\Delta\beta$ ($\Delta\beta\omega_0 \gg 1$), both \coth and \tanh functions saturate to value unity ($\Delta\beta\omega_0 \approx 6$) which implies that the TUR bound scales as $\Delta\beta\omega_0/2$ and the T-TUR will be satisfied. Therefore, along with the condition $\mathcal{T}_T(J) > 2/3$, the violation of T-TUR in this case requires a careful tuning of β_1 , β_2 , and ω_0 .

In Fig. 3(a) we display a two-dimensional plot for TUR as a function of $\beta_2\omega_0$ and JT . We set $\beta_1\omega_0 = 0$. Figure 3(b) is the corresponding binary plot differentiating the validity (dark red) and the violation regimes (blue) of the T-TUR. We clearly observe a regime for which T-TUR is not valid and the results nicely match with our theoretical predictions. As mentioned earlier, for sufficiently large $\Delta\beta$ ($\Delta\beta\omega_0 > 3.2$), the T-TUR bound is always satisfied. In contrast, the minimum value of the TUR bound is found to be ≈ 1.86 which occurs for a maximum transition probability $\mathcal{T}_T(J) = 1$, i.e., $JT = \pi/2$ and $\Delta\beta\omega_0 \approx 2.01$.

In Fig. 4 we show that the TUR bound obtained in Eq. (26) is in fact a tighter one compared to the generalized bound [Eqs. (2) and (3)]. More importantly, we observe that the generalized bound obtained from fluctuation symmetry becomes loose with increasing $\Delta\beta$ whereas the obtained bound closely follow the actual TUR trend. In fact, for large $\Delta\beta$, the net entropy production $\langle \Sigma \rangle$ scales as $\Delta\beta$; hence the G-TUR1 behaves as $2\langle \Sigma \rangle / e^{\langle \Sigma \rangle}$, which tends to zero, whereas the TUR bound obtained in Eq. (26) scales as $\Delta\beta\omega_0/2$. As expected, G-TUR2 performs a bit better than G-TUR1.

C. Hybrid spin-oscillator system

As a final toy model example we consider a hybrid system consisting of a single qubit and a single quantum harmonic oscillator [see Fig. 1(c)], once again interacting via a thermal coupling term. The total Hamiltonian is given as

$$H_{JC} = \frac{\omega_0}{2} \sigma_z \otimes 1_1 + 1_2 \otimes \omega_0 a^\dagger a + J (a^\dagger \otimes \sigma^- + a \otimes \sigma^+). \quad (27)$$

where $\sigma^\pm = \sigma_x \pm i\sigma_y$ are the spin ladder operators. This model is in fact the famous Jaynes-Cummings (JC) model and is one of the most well-studied setups in quantum optics. We are interested here to analyze the quantum thermodynamics properties for this model and compute the exact CGF for the energy exchange. We provide here a brief outline of the derivation.

Starting from Eq. (7) we switch to the interaction picture with respect to the bare part of the Hamiltonian [the first two

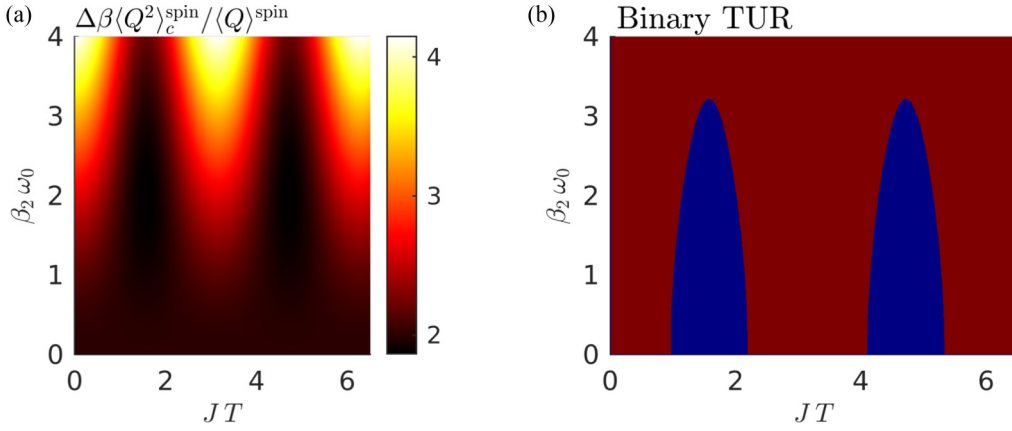


FIG. 3. (a) Two-dimensional plot for TUR ratio ($\Delta\beta \frac{\langle Q^2 \rangle_c^{\text{spin}}}{\langle Q \rangle_c^{\text{spin}}}$) for the coupled two-qubit system as a function of JT and $\beta_2\omega_0$. We set $\beta_1 = 0$. (b) Corresponding binary plot of TUR. The violation regime of the T-TUR bound is colored by blue (darker shed in grey scale) and the validity regime is colored by dark red.

terms of Eq. (27)] and compute the total unitary propagator in the qubit basis. We receive [88]

$$U_I(t) = e^{-iVt} = \begin{bmatrix} \cos(\sqrt{aa^\dagger}Jt) & -i\frac{\sin(\sqrt{aa^\dagger}Jt)}{\sqrt{aa^\dagger}}a \\ -i\frac{\sin(\sqrt{a^\dagger a}Jt)}{\sqrt{a^\dagger a}}a^\dagger & \cos(\sqrt{a^\dagger a}Jt) \end{bmatrix}, \quad (28)$$

where we have used the convention that $[U_I(t)]_{11} = \langle e|U_I(t)|e \rangle$, $[U_I(t)]_{12} = \langle e|U_I(t)|g \rangle$, $[U_I(t)]_{21} = \langle g|U_I(t)|e \rangle$, and $[U_I(t)]_{22} = \langle g|U_I(t)|g \rangle$. Note that because of the commutable coupling condition, in the interaction picture, the time-ordered operator in the unitary propagator does not play any role. With the help of this exact unitary operator and carrying out the calculation in the qubit basis, the exact CGF

can be written down as

$$\mathcal{G}_T^{\text{JC}}(u) = \ln \left[1 + \mathcal{Q} \left\{ \frac{f_1}{n_2} (e^{iu\omega_0} - 1) + \frac{(1-f_1)}{(1+n_2)} (e^{-iu\omega_0} - 1) \right\} \right], \quad (29)$$

where we define the function $\mathcal{Q} = \mathcal{Q}(J, T, \omega_0; \beta_2)$ as

$$\mathcal{Q}(J, T, \omega_0; \beta_2) = \sum_{n=0}^{\infty} e^{-\beta_2 n \omega_0} \sin^2(\sqrt{n}JT). \quad (30)$$

We make the following observations here:

(i) Unlike the coupled oscillator or the coupled qubit model, for this hybrid setup the transition probability is weighted by the oscillator temperature β_2 as captured by the \mathcal{Q} function.

(ii) Because of the hybrid nature of the setup both the Fermi-like and the Bose functions appear in the CGF expression.

Once again, it is easy to check the validity of the XFT for arbitrary J, T and the initial temperatures β_1, β_2 . Note that in the low-temperature limit of the oscillator, i.e., $\beta_2\omega_0 \gg 1$, it is expected that the above result should reproduce the two-qubit CGF. This can be seen as follows: for $\beta_2\omega_0 \gg 1$ only the $n = 1$ term contributes to Eq. (30). Therefore, the \mathcal{Q} function simplifies to $\mathcal{Q} \approx e^{-\beta_2\omega_0} \sin^2(JT)$ and correspondingly the Bose functions simplify to $n_2 \approx e^{-\beta_2\omega_0} (1 + e^{-\beta_2\omega_0})$ and $1 + n_2 \approx 1 + e^{-\beta_2\omega_0}$ which gives $\mathcal{Q}/n_2 = (1 - f_2) \sin^2(JT)$ and $\mathcal{Q}/(1 + n_2) = f_2 \sin^2(JT)$ and thus one correctly recovers the two-qubit model CGF, given in Eq. (17).

We now investigate the TUR bound and write down the cumulants as

$$\langle Q \rangle^{\text{JC}} = \omega_0 \mathcal{Q} \left(\frac{f_1}{n_2} - \frac{1-f_1}{1+n_2} \right) = \omega_0 \mathcal{Q} \frac{f_1}{1+n_2} (e^{\beta_2\omega_0} - e^{\beta_1\omega_0}), \quad (31)$$

$$\langle Q^2 \rangle^{\text{JC}} = \omega_0^2 \mathcal{Q} \left[\left(\frac{f_1}{n_2} + \frac{1-f_1}{1+n_2} \right) - \mathcal{Q} \left(\frac{f_1}{n_2} - \frac{1-f_1}{1+n_2} \right)^2 \right]. \quad (32)$$

As expected, the energy exchange in Eq. (31) vanishes when both the spin and the oscillator are initially kept at the same temperature. Interestingly, we once again receive a similar

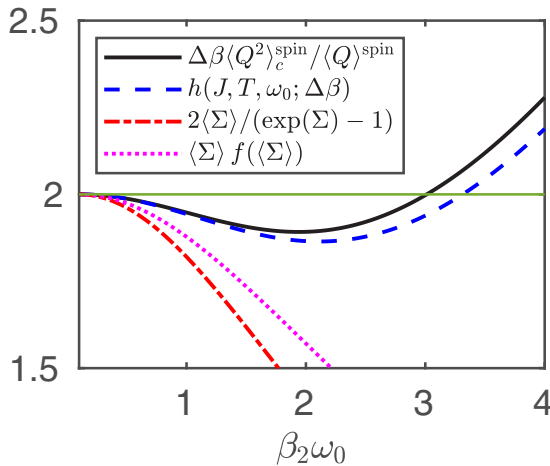


FIG. 4. Comparison between the TUR bounds obtained in Eq. (26) (blue dashed line), denoted here by $h(J, T, \omega_0; \Delta\beta) = \Delta\beta\omega_0 [\coth \frac{\Delta\beta\omega_0}{2} - \frac{T_T(J)}{2} \tanh \frac{\Delta\beta\omega_0}{2}]$, the generalized bounds, GTUR-1 (red dash-dotted line) in Eq. (2), and GTUR-2 (magenta dotted line) in Eq. (3) with the actual TUR value (black solid line). For reference a line is drawn at the value 2. The parameters are $\beta_1\omega_0 = 0.1$ and $JT = \pi/2$. The bound in Eq. (26) closely follows the actual TUR trend.

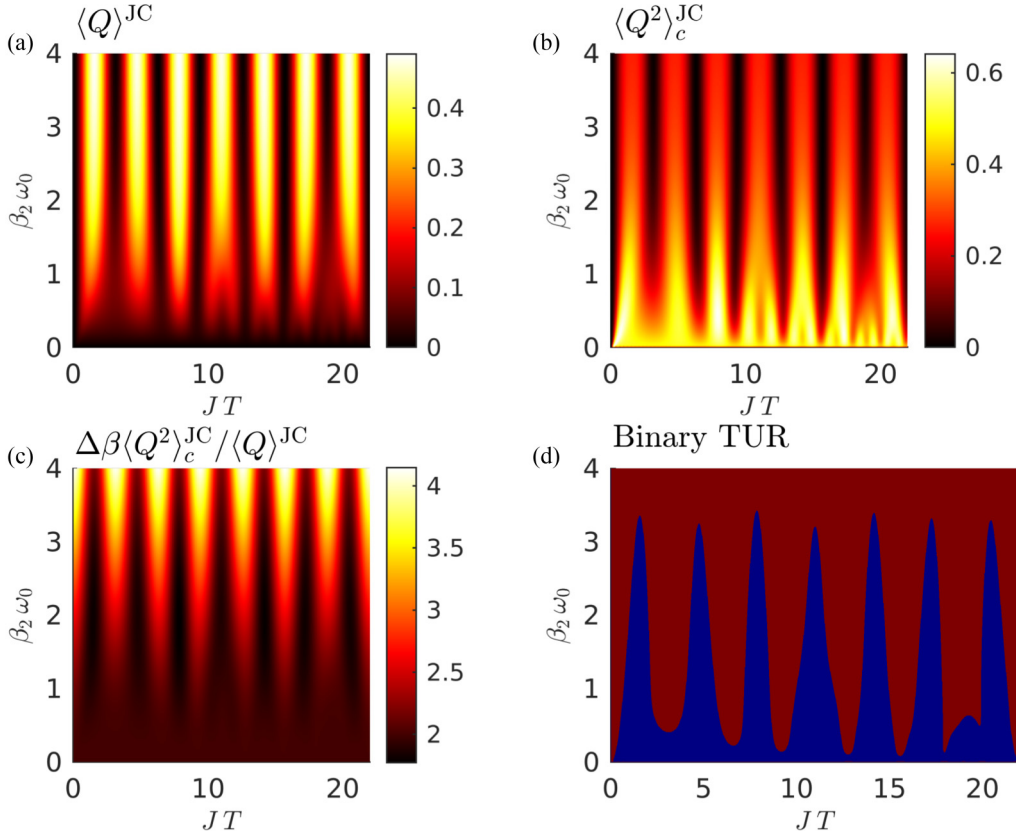


FIG. 5. Two-dimensional plots for the JC model: (a) average energy change $\langle Q \rangle^{JC}$, (b) corresponding noise $\langle Q^2 \rangle_c^{JC}$, (c) the TUR ratio $\Delta\beta \frac{\langle Q^2 \rangle_c^{JC}}{\langle Q \rangle^{JC}}$, and (d) binary plot of the same TUR data where the violation regime of the T-TUR bound is colored by blue (darker shed in grey scale) and the validity regime is colored by dark red, as a function of JT and $\beta_2 \omega_0$. We set $\beta_1 = 0$.

identity as in Eq. (14) but now involving both the Fermi and Bose functions,

$$\begin{aligned} & f_1(1+n_2) + n_2(1-f_1) \\ &= \coth \left[\frac{\Delta\beta\omega_0}{2} \right] (f_1(1+n_2) - n_2(1-f_1)), \end{aligned} \quad (33)$$

which helps us to write the TUR ratio as

$$\Delta\beta \frac{\langle Q^2 \rangle_c^{JC}}{\langle Q \rangle^{JC}} = \Delta\beta\omega_0 \coth \frac{\Delta\beta\omega_0}{2} - \langle \Sigma \rangle^{JC}. \quad (34)$$

This expression once again should be compared with Eq. (15) and Eq. (21). Interestingly, analogous to the previous cases, the first term remains the same, whereas the average entropy production term for the hybrid case produces a negative contribution to the TUR ratio, as was the case for the two-qubit model. Therefore, the breakdown of the T-TUR bound can be expected even for this setup. However, note that, in the limit when $Q \ll 1$, i.e., in the weak-coupling limit, the T-TUR is once again preserved. In Sec. IV we provide a general proof for the T-TUR bound for any two weakly coupled systems and extend the general analysis to the steady-state regime as well.

In Fig. 5 we display the two-dimensional plots for the first and second cumulant and the corresponding TUR ratio. Notice that the cumulants and the corresponding TUR ratio are not entirely periodic as a function of JT , especially in the high-temperature regime $\beta_2 \omega_0 \ll 1$. This is clear from

the expression for the function Q . The violation for the T-TUR bound is clearly observed in the binary plot [Fig. 5(d)]. Expectedly, the low-temperature behavior for the TUR ratio is found to be similar with the two-qubit case with clear validity of the T-TUR bound beyond $\Delta\beta\omega_0 \approx 3.4$. However, in the high-temperature regime the violation regime for the JC model is broader [comparing TUR ratio vs JT within the first period in both Fig. 3(b) and Fig. 5(d)] in comparison to the two-qubit case. This is because of the availability of many states for the oscillator leading a significant contribution of the average entropy production.

IV. PROOF OF T-TUR IN THE WEAK-COUPLING REGIME

In this section, we provide the key steps for the proof of the tighter bound of TUR (T-TUR) [Eq. (1)] in the weak-coupling regime for generic bipartite setups that are initially equilibrated in their respective thermal state. The primary task here is to obtain a general expression for the CGF in the weak-coupling limit. In Appendix B, we provide a detailed derivation for the same following the Keldysh nonequilibrium Green's function approach. Here we give out the main results.

Keeping the general situation in mind, we consider two systems with arbitrary Hamiltonians H_1 and H_2 with each system initially equilibrated to a thermal equilibrium state at a particular temperature. The initial composite density matrix is then given as, $\rho(0) = \rho_1 \otimes \rho_2 = \frac{e^{-\beta_1 H_1}}{\mathcal{Z}_1} \otimes \frac{e^{-\beta_2 H_2}}{\mathcal{Z}_2}$. A coupling

between the system is suddenly turned on and a general form for the coupling is chosen as $V = JA \otimes B$, where A (B) is an Hermitian operator involving system 1 (system 2). In the weak-coupling limit an analytical expression for the CGF can be obtained (please see Appendix B for a rigorous derivation) and is given as

$$\chi_T(u) = -\frac{J^2}{2} \int_{-\infty}^{\infty} \frac{d\omega_1}{2\pi} \int_{-\infty}^{\infty} \frac{d\omega_2}{2\pi} \mathcal{F}(\omega_1, \omega_2; T) [g_A^<(\omega_1)g_B^>(\omega_2)(e^{iu\omega_1} - 1) + g_A^>(\omega_1)g_B^<(\omega_2)(e^{-iu\omega_1} - 1)], \quad (35)$$

where $\mathcal{F}(\omega_1, \omega_2; T) = \frac{\sin^2 \left[\frac{(\omega_1 - \omega_2)T}{2} \right]}{(\omega_1 - \omega_2)^2}$, and $g_{A,B}^{<,>}$ are the lesser (<) and the greater (>) components of the bare Green's function. In the time domain these functions are given as $g_X^>(t_1, t_2) = -i \langle X(t_1)X(t_2) \rangle$ and $g_X^<(t_1, t_2) = -i \langle X(t_2)X(t_1) \rangle$, $X = A, B$, with average taken over the respective equilibrium canonical density operator. To arrive at Eq. (35) we have used only a weak-coupling approximation. However, this does not automatically ensure current conservation or the XFT as can be seen from Eq. (35). In order to meet these criteria one needs to further impose a resonant condition for energy exchange. We therefore use many-body quantum state representation for the individual system Hamiltonians H_1 and H_2 , and write the lesser and greater components of the Green's functions explicitly. For system 1,

$$g_A^<(t) = -i \sum_{mn} \frac{e^{-\beta_1 E_m}}{Z_A} |A_{m,n}|^2 e^{i\omega_{nm}t}, \quad (36)$$

$$g_A^>(t) = -i \sum_{mn} \frac{e^{-\beta_1 E_m}}{Z_A} |A_{m,n}|^2 e^{-i\omega_{nm}t},$$

where $\omega_{nm} = E_n - E_m$, $|A_{mn}|^2 = |\langle m|A|n \rangle|^2$ with $|m\rangle, |n\rangle$ being the energy eigenstates for system 1 with Hamiltonian H_1 and E_m, E_n are the corresponding eigenvalues. One receives a similar expression for $g_B^{<,>}(t)$ but with inverse temperature β_2 . We denote the corresponding energy eigenstates with $|p\rangle, |q\rangle$. Using a Fourier-transformed version of these Green's functions and taking first derivative with respect to iu of Eq. (35) we receive the expression for the average energy change,

$$\langle Q \rangle = 2\pi^2 J^2 \sum_{mn} \sum_{pq} \omega_{mn} \mathcal{F}(\omega_{mn}, \omega_{qp}; T) |A_{mn}|^2 |B_{pq}|^2 \times [e^{-\beta_1 \omega_{mn}} e^{\beta_2 \omega_{qp}} - 1] \frac{e^{-\beta_1 E_m}}{Z_A} \frac{e^{-\beta_2 E_p}}{Z_B}. \quad (37)$$

We now impose the resonant energy exchange condition between the two systems, which implies $E_m - E_n \approx E_q - E_p$, i.e., $\omega_{mn} \approx \omega_{qp}$ leading to $\mathcal{F}(\omega_{mn}, \omega_{qp}; T) \approx T^2$, and we receive

$$\langle Q \rangle = 2\pi^2 J^2 T^2 \sum_{mn} \sum_{pq} \omega_{mn} |A_{mn}|^2 |B_{pq}|^2 \times [e^{\Delta\beta \omega_{qp}} - 1] \frac{e^{-\beta_1 E_m}}{Z_A} \frac{e^{-\beta_2 E_p}}{Z_B}. \quad (38)$$

Using the same resonant condition, we receive for the noise from Eq. (35)

$$\begin{aligned} \langle Q^2 \rangle_c &= 2\pi^2 J^2 T^2 \sum_{mn} \sum_{pq} \omega_{mn}^2 |A_{mn}|^2 |B_{pq}|^2 \frac{e^{-\beta_1 E_m}}{Z_A} \frac{e^{-\beta_2 E_p}}{Z_B} \\ &\quad \times [e^{\Delta\beta \omega_{qp}} + 1] \quad (39) \\ &= 2\pi^2 J^2 T^2 \sum_{mn} \sum_{pq} \omega_{mn} |A_{mn}|^2 |B_{pq}|^2 \frac{e^{-\beta_1 E_m}}{Z_A} \frac{e^{-\beta_2 E_p}}{Z_B} \\ &\quad \times \omega_{qp} \coth \left[\frac{\Delta\beta \omega_{qp}}{2} \right] [e^{\Delta\beta \omega_{qp}} - 1], \\ &\geq \frac{2}{\Delta\beta} \langle Q \rangle, \quad (40) \end{aligned}$$

where going from the first to the third line we write $\omega_{mn}^2 \approx \omega_{mn} \omega_{qp}$ by making use of the resonant condition. Notice the important term $\omega_{qp} \coth \left[\frac{\Delta\beta \omega_{qp}}{2} \right]$ in the fourth line, which is always greater than or equal to $2/\Delta\beta$, using which we receive the T-TUR bound. Also, note that the cumulants in this limit scale with T^2 and the entire analysis remains valid for $JT \ll 1$.

The another key importance of the expression in Eq. (35) is that one can readily discuss results for the long-time limit $T \rightarrow \infty$. In fact, if a unique long-time limit of Eq. (35) exists that supports a nonequilibrium steady state for the bipartite setup (imagining each system to be macroscopic bath), in this case all cumulants scale with T , as

$$\lim_{T \rightarrow \infty} \frac{\sin^2 \left[\frac{(\omega_1 - \omega_2)T}{2} \right]}{\frac{(\omega_1 - \omega_2)^2}{4}} = 2\pi T \delta(\omega_1 - \omega_2), \quad (41)$$

and one receives the following expressions for the cumulants following Eq. (35):

$$\begin{aligned} \frac{\langle Q \rangle}{T} &= -J^2 \int_{-\infty}^{\infty} \frac{d\omega}{4\pi} \omega g_A^>(\omega) g_B^<(\omega) [e^{\Delta\beta \omega} - 1], \quad (42) \\ \frac{\langle Q^2 \rangle_c}{T} &= -J^2 \int_{-\infty}^{\infty} \frac{d\omega}{4\pi} \omega^2 g_A^>(\omega) g_B^<(\omega) [e^{\Delta\beta \omega} + 1] \\ &= -J^2 \int_{-\infty}^{\infty} \frac{d\omega}{4\pi} \omega^2 \coth[\Delta\beta \omega/2] g_A^>(\omega) g_B^<(\omega) \\ &\quad \times [e^{\Delta\beta \omega} - 1], \\ &\geq -\frac{2}{\Delta\beta} J^2 \int_{-\infty}^{\infty} \frac{d\omega}{4\pi} \omega g_A^>(\omega) g_B^<(\omega) [e^{\Delta\beta \omega} - 1] \\ &\geq \frac{2}{\Delta\beta} \frac{\langle Q \rangle}{T}, \quad (43) \end{aligned}$$

where once again, like in the previous case, in the third line of the $\langle Q^2 \rangle_c/T$ expression we use the inequality $\omega \coth[\Delta\beta \omega/2] \geq 2/\Delta\beta$. Therefore, for a weakly coupled bipartite setup in the steady state the T-TUR is preserved. It is crucial to note that both the G-TUR1 and G-TUR2 in this long-time limit fail to predict any nontrivial bound for the TUR ratio as the average entropy production $\langle \Sigma \rangle$ diverges as $T \rightarrow \infty$.

V. SUMMARY

We examined the TUR bound for energy exchange for three simple model systems characterized by different underlying statistics for the transport carriers. We obtained exact analytical expressions for the heat exchange characteristic function for all three cases which hands over the cumulants to analyze the TUR. One of the interesting observations was the similarity in the expressions for the CGF for the two-qubit and two-oscillator model where they differ by crucial sign differences arising from the underlying Fermi-like and the Bose statistics. We found that, in general, the TUR ratio is sensitive to the statistics and the validity or violation of the T-TUR is critically dependent on this. In all three cases, interestingly, the TUR ratio was organized in terms of a universal term which is always greater than or equal to 2 and a net entropy production term. The deviation from the T-TUR bound largely depends on the contribution of this average entropy production to the TUR ratio. For a coupled oscillator system, displaying pure bosonic statistics, this contribution turned out to be always positive and thus the tighter bound is always preserved. In contrast, the appearance of the Fermi-like statistics for both the qubit and the hybrid model leads to a negative contribution, leading to a lower bound (smaller than the T-TUR) for the TUR. However, in the weak-coupling regime, all these models satisfy the T-TUR bound. We provide a rigorous proof for the T-TUR, in the weak-coupling regime, by deriving a general expression for the CGF following the NEGF approach. Future work will direct towards designing finite-time heat engine cycles based on these toy models and understanding the impact of the statistics on the engine efficiency and the corresponding TUR bound.

ACKNOWLEDGMENTS

B.K.A. gratefully acknowledges the financial support from Max Planck-India mobility grant. B.K.A. thanks D. Segal for useful discussions. S.S. acknowledges support from the Council of Scientific & Industrial Research (CSIR), India (Grant No. 1061651988). O.S. acknowledges the Inspire grant from the Department of Science & Technology (DST), India.

APPENDIX A: EXCHANGE FLUCTUATION THEOREM (XFT) UNDER COMMUTABLE COUPLING CONDITION

In this Appendix we prove that for a bipartite setup under the thermal coupling limit the XFT is valid for arbitrary coupling strength between two systems and for arbitrary time duration of energy exchange. The starting point here is the CF for energy exchange, given in Eq. (7):

$$\chi_T(u) = \text{Tr}[\mathcal{U}^\dagger(T, 0)(e^{-iuH_1} \otimes 1_2)\mathcal{U}(T, 0)(e^{iuH_1} \otimes 1_2)\rho(0)], \quad (\text{A1})$$

where $\mathcal{U}(t, 0) = e^{-iHt}$ is the global unitary operator with $H = H_1 + H_2 + V$. To take advantage of the thermal coupling limit, i.e., the commutable coupling condition $[H_1 + H_2, V] = 0$, one can rewrite the above expression along with the consideration that initially both the systems are in their respective Gibbs thermal state, i.e., $\rho(0) = \frac{e^{-\beta_1 H_1}}{\mathcal{Z}_1} \otimes \frac{e^{-\beta_2 H_2}}{\mathcal{Z}_2}$, which further

implies $[\rho(0), H_1] = 0$. One then receives

$$\chi_T(u) = \frac{1}{\mathcal{Z}_1 \mathcal{Z}_2} \text{Tr}[(e^{iuH_1} \otimes 1_2) e^{\Delta\beta H_1} e^{-\beta_2(H_1+H_2)} \mathcal{U}^\dagger(T, 0) \times (e^{-iuH_1} \otimes 1_2) \mathcal{U}(T, 0)], \quad (\text{A2})$$

where recall that $\Delta\beta = \beta_2 - \beta_1$. The thermal coupling condition allows swapping the third and fourth terms. Next, performing cyclic permutation under the trace operation, we receive

$$\chi_T(u) = \frac{1}{\mathcal{Z}_1 \mathcal{Z}_2} \text{Tr}[\mathcal{U}(T, 0)(e^{-i(-u+i\Delta\beta)H_1} \otimes 1_2) \times \mathcal{U}^\dagger(T, 0)(e^{i(-u+i\Delta\beta)H_1} \otimes 1_2) \rho(0)], \quad (\text{A3})$$

where $\Delta\beta = \beta_2 - \beta_1$. This expression still does not give us the XFT that we are looking for. In fact, at this point the above expression satisfies a fluctuation relation given as $\chi_T(u) = \chi_{-T}(-u + i\Delta\beta)$ connecting forward and reversed protocol.

In order to proceed, we now assume that the composite and the individual systems are time-reversal invariant, which is the case considered in this paper. We then have $\Theta \mathcal{U}(T, 0) = \mathcal{U}^\dagger(T, 0) \Theta$, $\Theta e^{-iuH_1} = e^{iu^*H_1} \Theta$ and $[\Theta, H_{1,2}] = 0$. Θ is the time-reversal operator. Now inserting $\Theta^{-1}\Theta$ inside the trace and using Eq. (A2) we receive

$$\begin{aligned} \chi_T(u) &= \frac{1}{\mathcal{Z}_1 \mathcal{Z}_2} \text{Tr}[\Theta^{-1} \Theta \mathcal{U}(T, 0)(e^{-i(-u+i\Delta\beta)H_1} \otimes 1_2) \\ &\quad \times \mathcal{U}^\dagger(T, 0)(e^{i(-u+i\Delta\beta)H_1} \otimes 1_2) \rho(0)], \\ &= \frac{1}{\mathcal{Z}_1 \mathcal{Z}_2} \text{Tr}[\Theta^{-1} \mathcal{U}^\dagger(T, 0)(e^{i(-u^*-i\Delta\beta)H_1} \otimes 1_2) \\ &\quad \times \mathcal{U}(T, 0)(e^{-i(-u^*-i\Delta\beta)H_1} \otimes 1_2) \rho(0) \Theta]. \end{aligned} \quad (\text{A4})$$

Now due to the antilinear nature of Θ we have $\text{Tr}[\Theta^{-1} A \Theta] = \text{Tr}[A^\dagger]$ [11]. Therefore, we finally receive

$$\begin{aligned} \chi_T(u) &= \frac{1}{\mathcal{Z}_1 \mathcal{Z}_2} \text{Tr}[\mathcal{U}^\dagger(T, 0)(e^{-i(-u+i\Delta\beta)H_1} \otimes 1_2) \\ &\quad \times \mathcal{U}(T, 0)(e^{i(-u+i\Delta\beta)H_1} \otimes 1_2) \rho(0)] \\ &= \chi_T(-u + i\Delta\beta) \end{aligned} \quad (\text{A5})$$

for arbitrary time duration T and coupling strength.

APPENDIX B: DERIVATION OF THE CGF IN EQ. (35) IN THE WEAK-COUPLING REGIME

In this Appendix we provide the derivation for the CGF in Eq. (35) following the Keldysh nonequilibrium Green's function approach [78–80]. This method turned out to be useful to receive bounds in transient as well as in the steady-state regime, as shown in Sec. IV. We begin with Eq. (7) and organize the characteristic function in the interaction picture as

$$\begin{aligned} \chi_T(u) &= \int dQ e^{iuQ} p_T(Q), \\ &= \text{Tr}[\mathcal{U}_I^\dagger(T, 0)(e^{-iuH_1} \otimes 1_2) \mathcal{U}_I(T, 0)(e^{iuH_1} \otimes 1_2) \rho(0)], \end{aligned}$$

where $\mathcal{U}_I(t, 0) = \mathcal{T} \exp[-i \int_0^t V_I(t') dt']$ with \mathcal{T} being the time-ordered operator and $V_I(t) = e^{iH_0 t} V e^{-iH_0 t}$, $H_0 = H_1 + H_2$. Recall that the composite density matrix is decoupled at

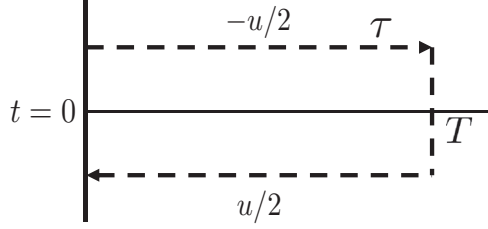


FIG. 6. The complex time Keldysh contour with upper and lower branch. The contour path begins from $t = 0$, goes to maximum time $t = T$, and then comes back to $t = 0$ again. The upper (lower) branch corresponds to a time-ordered forward (anti-time-ordered backward) evolution propagator. For the energy counting statistics problem the Hamiltonian is dressed differently in the upper ($-u/2$) and the lower ($+u/2$) branches by the counting parameter u . τ is the contour-time parameter.

the initial time $t = 0$ with each system in thermal equilibrium at a particular temperature, i.e., $\rho(0) = \rho_1 \otimes \rho_2 = \frac{e^{-\beta_1 H_1}}{\mathcal{Z}_1} \otimes \frac{e^{-\beta_2 H_2}}{\mathcal{Z}_2}$. This condition implies $[\rho(0), H_0] = 0$. Then the above equation can be organized as

$$\chi_T(u) = \text{Tr}[\rho(0)[U_I^\dagger]^{u/2}(T, 0)U_I^{-u/2}(T, 0)], \quad (\text{B1})$$

where now both the forward and backward evolution operators are dressed by the counting field u . This expression can be recast on a Keldysh contour as (see Fig. 6)

$$\chi_T(u) = \text{Tr}[\rho(0)T_c e^{-i \int_c V_i^x(\tau) d\tau}], \quad (\text{B2})$$

where T_c is the contour-ordered operator, which orders operators according to their contour time argument: an earlier (later) contour time places the operator to the right (left). Therefore, the upper (lower) branch corresponds to the forward (backward) evolution. $x(\tau)$ is a contour-time-dependent function which can take two possible values depending on the location of τ on the contour branch. Here $x^+(t) = -u/2$ for the upper branch (denoted by the $+$ sign) and $x^-(t) = u/2$ for the lower branch (denoted by the $-$ sign) within the measurement time interval $[0, \tau]$. $x^\pm(t) = 0$ outside the measurement time. Finally $V_I^x(\tau) = e^{ixH_1} V_I(\tau) e^{-ixH_1}$ is the modified contour-time-dependent operator dressed by the counting field.

Often, instead of the CF, it is more convenient to work with the logarithm of the characteristic function $\mathcal{G}_T(u) \equiv \ln \chi_T(u)$ which according to the linked-cluster theorem [81] contains only the connected diagrams. Since our focus is on the weak-coupling regime, we therefore expand the exponential and collect terms up to the leading order in the coupling V that produce nonzero contribution. It turns out that the first-order contribution in V vanishes. This can be shown as follows: The CGF in the first order, denoted by $\mathcal{G}_T^{(1)}(u)$, is given as

$$\mathcal{G}_T^{(1)}(u) = -i \int d\tau \langle V_I^x(\tau) \rangle = -i \int_0^T dt [\langle V_I^{x^+}(t) \rangle - \langle V_I^{x^-}(t) \rangle], \quad (\text{B3})$$

where in the second line we transform back to the real time (t) from the contour time (τ) using the Langreth rule [80,82]. Note that in this order the contour-ordered

operator does not play any role. Now since $V_I^{x^\pm}(t_1) = e^{\mp i\xi/2H_1} V_I(t_1) e^{\mp i\xi/2H_1}$ and furthermore because $[\rho(0), H_1] = 0$, the counting-field-dependent phase factors cancel out exactly, leaving $\langle V_I^{x^+}(t) \rangle = \langle V_I^{x^-}(t) \rangle$, i.e., independent of the branch index, and thus the above contribution vanishes.

Next, the second-order contribution to the CGF is given as

$$\begin{aligned} \mathcal{G}_T^{(2)}(u) &= \frac{(-i)^2}{2} \int d\tau_1 \int d\tau_2 \langle T_c V_I^x(\tau_1) V_I^x(\tau_2) \rangle_c \\ &= \int d\tau_1 \int d\tau_2 \tilde{\mathcal{G}}_c(\tau_1, \tau_2), \end{aligned} \quad (\text{B4})$$

where $\tilde{\mathcal{G}}_c(\tau_1, \tau_2)$ indicates the connected part of the correlation function with the tilde symbol referring to the counting field dependence. Since the normalization condition demands that $\mathcal{G}_T^{(2)}(u = 0) = 0$, one can explicitly enforce the normalization in the above expression as

$$\mathcal{G}_T^{(2)}(u) = \int d\tau_1 \int d\tau_2 [\tilde{\mathcal{G}}_c(\tau_1, \tau_2) - G_c(\tau_1, \tau_2)], \quad (\text{B5})$$

where recall that Green's functions without the tilde symbol refer to $u = 0$. We once again transform back to the real time following the same procedure as mentioned earlier and obtain

$$\begin{aligned} \mathcal{G}_T^{(2)}(u) &= \int_0^T dt_1 \int_0^T dt_2 [G_c^<(t_1, t_2) + G_c^>(t_1, t_2) \\ &\quad - \tilde{\mathcal{G}}_c^<(t_1, t_2) - \tilde{\mathcal{G}}_c^>(t_1, t_2)], \end{aligned} \quad (\text{B6})$$

where $< (>)$ corresponds to the lesser (greater) component of the Green's function. In order to proceed from here, we choose a generic form for the coupling, given as $V = JA \otimes B$, where A (B) corresponds to the Hermitian operator involving system 1 (system 2). For simplicity, we consider a single degree of freedom and systems with bosonic degree of freedom. However, the calculation can be straightforwardly extended for fermionic as well as for hybrid systems. Now since the average in the Green's functions is taken over $\rho(0)$, i.e., a decoupled initial state, the connected part of the correlation function in the contour time reduces to

$$\tilde{\mathcal{G}}_c(\tau_1, \tau_2) = \frac{J^2}{2} \tilde{g}_A(\tau_1, \tau_2) g_B(\tau_2, \tau_1), \quad (\text{B7})$$

where $\tilde{g}_A(\tau_1, \tau_2) = -i \langle T_c A^x(\tau_1) A^x(\tau_2) \rangle$ is the bare but counting-field-dependent correlation function for system 1 with average taken over the equilibrium density operator $\rho_1 = \frac{e^{-\beta_1 H_1}}{\mathcal{Z}_1}$ and similarly $g_B(\tau_1, \tau_2) = -i \langle T_c B(\tau_1) B(\tau_2) \rangle$ with average taken over the equilibrium density operator $\rho_2 = \frac{e^{-\beta_2 H_2}}{\mathcal{Z}_2}$. Following Eq. (B5), in real time we are interested only in the lesser and the greater components, which are given as

$$\begin{aligned} \tilde{\mathcal{G}}_c^<(t_1, t_2) &= \frac{J^2}{2} g_A^<(t_1 - t_2 - u) g_B^>(t_2 - t_1), \\ \tilde{\mathcal{G}}_c^>(t_1, t_2) &= \frac{J^2}{2} g_A^>(t_1 - t_2 + u) g_B^<(t_2 - t_1). \end{aligned} \quad (\text{B8})$$

Since each of the bare Green's functions are time-translational invariant, we can work in the frequency domain by performing Fourier transformation, which gives

$$\chi_T(u) = -\frac{J^2}{2} \int_{-\infty}^{\infty} \frac{d\omega_1}{2\pi} \int_{-\infty}^{\infty} \frac{d\omega_2}{2\pi} \frac{\sin^2 \left[\frac{(\omega_1 - \omega_2)T}{2} \right]}{\frac{(\omega_1 - \omega_2)^2}{4}} [g_A^<(\omega_1)g_B^>(\omega_2)(e^{i\omega_1} - 1) + g_A^>(\omega_1)g_B^<(\omega_2)(e^{-i\omega_1} - 1)]. \quad (\text{B9})$$

Notice that since bare Green's functions are computed with respect to their respective equilibrium state, they follow the standard Kubo-Martin-Schwinger boundary condition [82] given as $g_A^>(\omega) = e^{\beta_1\omega} g_A^<(\omega)$ and, similarly for the system 2 Green's function, $g_B^>(\omega) = e^{\beta_2\omega} g_B^<(\omega)$. Using this condition, one can rewrite the expressions for first and second cumulant by taking the derivative of Eq. (B9) with respect to iu and receiving

$$\langle Q \rangle = -\frac{J^2}{2} \int_{-\infty}^{\infty} \frac{d\omega_1}{2\pi} \int_{-\infty}^{\infty} \frac{d\omega_2}{2\pi} \omega_1 \mathcal{F}(\omega_1, \omega_2; T) \times g_A^>(\omega_1)g_B^<(\omega_2)[e^{-\beta_1\omega_1} e^{\beta_2\omega_2} - 1], \quad (\text{B10})$$

$$\langle Q^2 \rangle_c = -\frac{J^2}{2} \int_{-\infty}^{\infty} \frac{d\omega_1}{2\pi} \int_{-\infty}^{\infty} \frac{d\omega_2}{2\pi} \omega_1^2 \mathcal{F}(\omega_1, \omega_2; T) \times g_A^>(\omega_1)g_B^<(\omega_2)[e^{-\beta_1\omega_1} e^{\beta_2\omega_2} + 1], \quad (\text{B11})$$

where we define $\mathcal{F}(\omega_1, \omega_2; T) = \frac{\sin^2 \left[\frac{(\omega_1 - \omega_2)T}{2} \right]}{\frac{(\omega_1 - \omega_2)^2}{4}}$. We use the above expressions to receive the T-TUR bound.

APPENDIX C: DERIVATION OF THE EXACT CGF FOR THE TWO-OSCILLATOR SYSTEM

In this Appendix we provide the derivation for the exact CGF given in Eq. (9). We once again employ the Keldysh nonequilibrium Green's function approach to derive the CGF. Note that this powerful approach can be extended to study bilinear systems with arbitrary complexity (see Ref. [74] for details). As before, we map the CF on the Keldysh contour in the interaction picture with respect to the bare part of the total Hamiltonian $H_0^{\text{osc}} = \hbar\omega_0 a_1^\dagger a_1 \otimes I_2 + I_1 \otimes \hbar\omega_0 a_2^\dagger a_2$ as

$$\chi_T(u) = \text{Tr}[\rho(0)T_c e^{-i \int_c V^x(\tau) d\tau}], \quad (\text{C1})$$

where the interaction Hamiltonian in this case is dressed as $V^x = e^{ixH_1} V e^{-ixH_1} = J(a_1^{x\dagger} a_2 + \text{H.c.})$, $x = \pm u/2$, affecting only the system 1 operators. Note that the operator V^x is time independent even in the interaction picture due to the commutable coupling symmetry. However, in Eq. (C1) we explicitly write the contour-ordered operator to keep track of the forward and the backward evolution. Recall that the contour-time variable τ runs from $[0, T]$. Invoking the linked-cluster theorem for the CGF $\mathcal{G}_T^{\text{osc}}(u) = \ln \chi_T(u)$ we receive a formal exact expression for the model in contour time τ as

$$\mathcal{G}_T^{\text{osc}}(u) = -\text{Tr}_\tau \ln [1 - g_{22} \Sigma_{11}^x]. \quad (\text{C2})$$

Here the Green's functions are understood as matrices in discretized contour time. In the continuous-time version the trace operation means $\text{Tr}_\tau[AB] = \int d\tau \int d\tau' A(\tau, \tau')B(\tau', \tau)$. In the above expression, following the standard notations for the Green's functions, we define

$$g_{ii}(\tau, \tau') = -i \langle T_c a_i(\tau) a_i^\dagger(\tau') \rangle, \quad i = 1, 2, \quad (\text{C3})$$

$$g_{ii}^x(\tau, \tau') = -i \langle T_c a_i^x(\tau) a_i^{x\dagger}(\tau') \rangle, \quad i = 1, 2 \quad (\text{C4})$$

as the bare [Eq. (C3)] and the counting-field-dependent [Eq. (C4)] Green's function, respectively. Recall that the counting field appears only for system 1 operators. The self-energy term is then given as $\Sigma_{11}^x(\tau, \tau') = J^2 g_{11}^x(\tau, \tau')$ with J being the coupling strength between the oscillators. Since $a_1^x(\tau) = e^{ixH_1} a_1(\tau) e^{-ixH_1} = a_1(\tau + x(\tau))$, it is thus clear that the effect of measuring or counting energy leads to a shift in contour time and correspondingly the self-energy is shifted as

$$\Sigma_{11}^x(\tau, \tau') = \Sigma_{11}(\tau + x(\tau), \tau' + x(\tau')). \quad (\text{C5})$$

Equation (C2) does not explicitly satisfy the normalization condition $\mathcal{G}_T^{\text{osc}}(u=0) = 0$. To enforce this condition, one can further simplify the above expression and write

$$\begin{aligned} 1 - g_{22} \Sigma_{11}^x &= g_{22}(g_{22}^{-1} - \Sigma_{11}^x) \\ &= g_{22}(g_{22}^{-1} - \Sigma - \Sigma_{11}^A) \\ &= g_{22}(G_{22}^{-1} - \Sigma_{11}^A) \\ &= g_{22} G_{22}^{-1} (1 - G_{22} \Sigma_{11}^A) \\ &= (1 - g_{22} \Sigma_{11})(1 - G_{22} \Sigma_{11}^A), \end{aligned} \quad (\text{C6})$$

where in the second line we define a useful quantity $\Sigma_{11}^A = \Sigma_{11}^x - \Sigma_{11}$ which is zero in the absence of the counting field. The third line motivates one to introduce a new Green's function $G_{22}^{-1} = g_{22}^{-1} - \Sigma_{11}$ which in the continuous-contour-time version satisfies the following Dyson equation:

$$G_{22}(\tau, \tau') = g_{22}(\tau, \tau') + \int_c \int_c d\tau_1 d\tau_2 g_{22}(\tau, \tau_1) \Sigma_{11}(\tau_1, \tau_2) \times G_{22}(\tau_2, \tau'). \quad (\text{C7})$$

Notice that this Green's function is nothing but the dressed Green's function of system 2, taking into account the presence of system 1 in terms of the self-energy Σ_{11} . With the help of Eq. (C6), Eq. (C2) then simplifies to

$$\mathcal{G}_T^{\text{osc}}(u) = -\text{Tr}_\tau \ln [1 - G_{22} \Sigma_{11}^A] \quad (\text{C8})$$

as $\text{Tr}_\tau \ln [1 - g_{22} \Sigma_{11}] = 0$ following Eq. (C2), ensuring the normalization condition. The next important task from here on is to go from the contour time to the real time following the Langreth theorem. Furthermore, a more transparent and simplified framework is obtained by performing an orthogonal Keldysh rotation (rotation in the space of real time by 45°) which gives

$$\mathcal{G}_T^{\text{osc}}(u) = -\text{Tr}_{r,\sigma} \ln [1 - \check{G}_{22} \check{\Sigma}_{11}^A]. \quad (\text{C9})$$

The breve symbol indicates that the Green's functions are written in the rotated Keldysh frame. Also note that the orthogonal Keldysh rotation preserves the trace in the above CGF expressions. In Eq. (C9) the meaning of trace is now in terms of the real time and, as well as over the branch index, denoted as σ . Explicitly, it means, for example, $\text{Tr}_{r,\sigma}[\check{A}\check{B}] =$

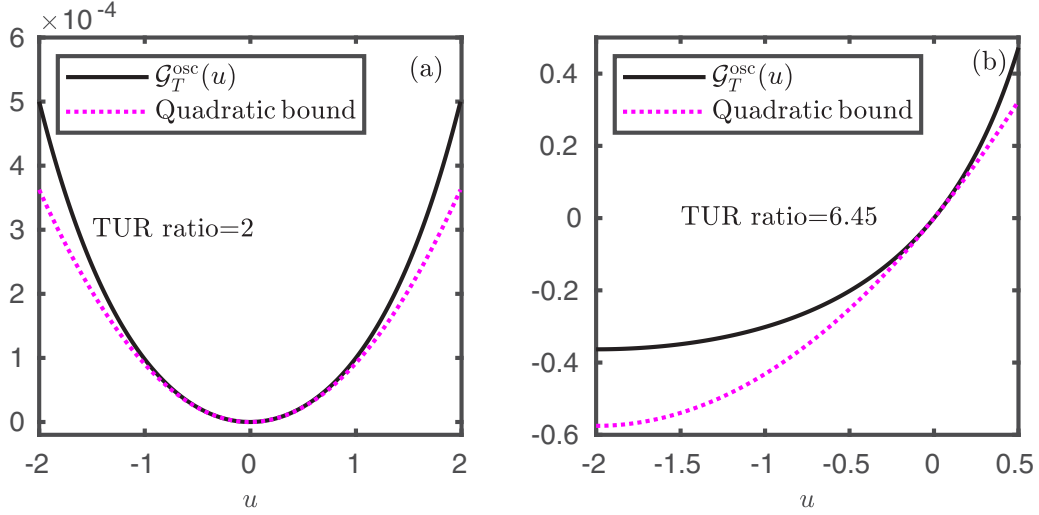


FIG. 7. Comparison between the exact CGF $\mathcal{G}_T^{\text{osc}}(u)$ in Eq. (9) and the quadratic CGF in Eq. (D1) for the two-oscillator problem for two different values for the TUR ratio: (a) TUR ratio = 2 and (b) TUR ratio = 6.45.

$\int_0^T dt_1 \int_0^T dt_2 \text{Tr}[\check{A}(t_1, t_2)\check{B}(t_2, t_1)]$. We receive the \check{G}_{22} as

$$\check{G}_{22} = \begin{bmatrix} G_{22}^r & G_{22}^k \\ 0 & G_{22}^a \end{bmatrix}, \quad (\text{C10})$$

where r , a , and k are the retarded, advanced, and the Keldysh components for the Green's function. These various components can be obtained exactly and are given as follows:

$$\begin{aligned} G_{22}^r(t, t') &= -i\theta(t-t')e^{-i\omega_0(t-t')} \cos(J(t-t')), \\ G_{22}^a(t, t') &= i\theta(t'-t)e^{-i\omega_0(t-t')} \cos(J(t-t')), \\ G_{22}^<(t, t') &= -i[n_2 \cos(Jt) \cos(Jt') + n_1 \sin(Jt) \sin(Jt')], \\ G_{22}^>(t, t') &= -i[(1+n_2) \cos(Jt) \cos(Jt') + (1+n_1) \\ &\quad \times \sin(Jt) \sin(Jt')], \end{aligned} \quad (\text{C11})$$

and the Keldysh component is given as $G_{22}^k = G_{22}^< + G_{22}^>$. Interestingly, the retarded and the advanced components are time-translational invariant which is not the case for the other components. It is easy to check that the lesser and

greater components satisfy the correct initial condition, given as $iG_{22}^<(t=t'=0) = \langle a_1^\dagger a_2 \rangle = n_2$ and $iG_{22}^>(t=t'=0) = \langle a_2 a_1^\dagger \rangle = (1+n_2)$. Similarly we receive for the counting-field-dependent self-energy

$$\check{\Sigma}_{11}^A = \frac{1}{2} \begin{bmatrix} a-b & a+b \\ -(a+b) & b-a \end{bmatrix}, \quad (\text{C12})$$

where

$$\begin{aligned} a &= \Sigma_{11}^>(t-t'+u) - \Sigma_{11}^>(t, t'), \\ b &= \Sigma_{11}^<(t-t'-u) - \Sigma_{11}^<(t, t'). \end{aligned} \quad (\text{C13})$$

The calculation further simplifies upon performing a two-time Fourier transformation, defined here as

$$\check{G}_{22}(\omega_1, \omega_2) = \int_0^T dt \int_0^T dt' e^{i\omega_1 t} e^{i\omega_2 t'} \check{G}_{22}(t, t'). \quad (\text{C14})$$

One then finally obtains from Eq. (C9)

$$\mathcal{G}_T^{\text{osc}}(u) = -\ln \det[1 - \check{G}_{22}(\omega_0, -\omega_0)\check{\Sigma}_{11}^A(\omega_0)]. \quad (\text{C15})$$

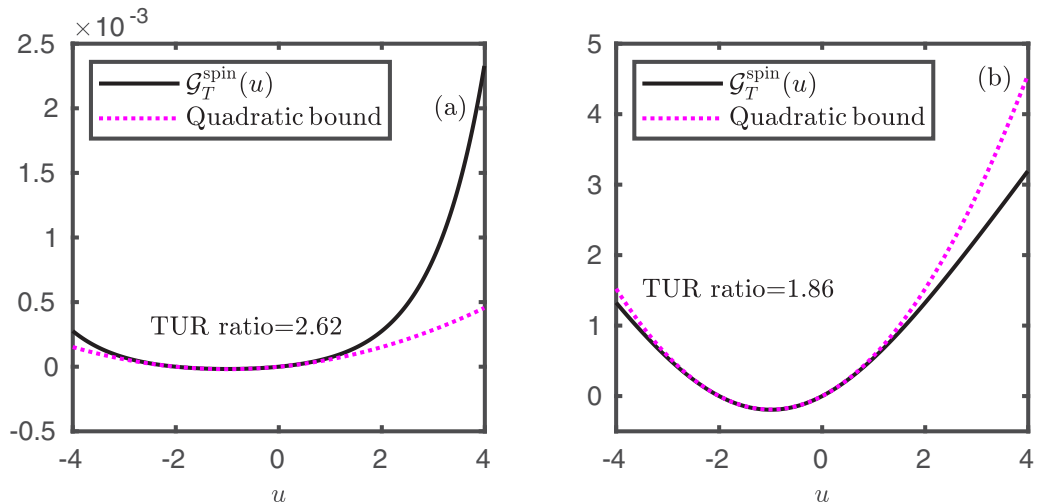


FIG. 8. Same as in Fig. 7 but for the two-qubit model with exact CGF for two different values for the TUR ratio: (a) TUR ratio = 2.62 and (b) TUR ratio = 1.86.

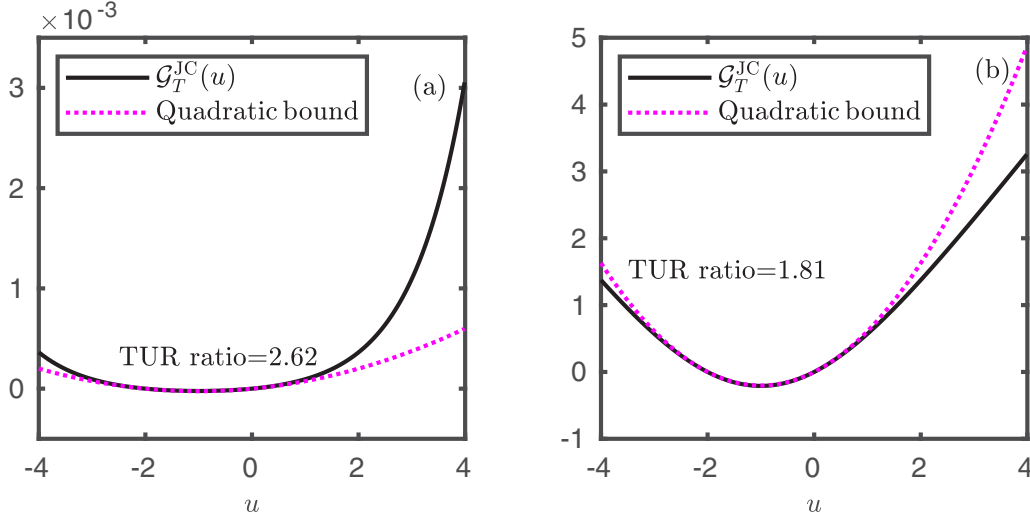


FIG. 9. Same as in Fig. 7 but for the hybrid spin-oscillator model for two different values for the TUR ratio: (a) TUR ratio = 2.62 and (b) TUR ratio = 1.81.

Note that the above formula is exact for arbitrary coupling J . This expression can be easily extended for a many-oscillator setup also. One can now write down the Fourier version of the Green's function components, which are given as

$$\begin{aligned}
 G_{22}^r(\omega_0, -\omega_0) &= -\frac{2i}{J^2} \sin^2\left(\frac{JT}{2}\right), \\
 G_{22}^a(\omega_0, -\omega_0) &= \frac{2i}{J^2} \sin^2\left(\frac{JT}{2}\right), \\
 G_{22}^<(\omega_0, -\omega_0) &= -\frac{i}{J^2} [n_2 \sin^2(JT) + n_1(1 - \cos(JT))^2], \\
 G_{22}^>(\omega_0, -\omega_0) &= -\frac{i}{J^2} [(1 + n_2) \sin^2(JT) + (1 + n_1) \\
 &\quad \times (1 - \cos(JT))^2], \quad (C16)
 \end{aligned}$$

and similarly for the self-energy components,

$$\begin{aligned}
 a &= \Sigma_{11}^>(\omega_0) (e^{-iu\hbar\omega_0} - 1) \\
 &= -iJ^2 (1 + n_1(\omega_0)) (e^{-iu\hbar\omega_0} - 1), \quad (C17)
 \end{aligned}$$

$$b = \Sigma_{11}^<(\omega_0) (e^{iu\hbar\omega_0} - 1) = -iJ^2 n_1(\omega_0) (e^{iu\hbar\omega_0} - 1). \quad (C18)$$

Knowing these analytical expressions for the Green's functions one can simply compute the determinant in Eq. (C15), which finally gives the CGF expression in Eq. (9).

APPENDIX D: COMPARISON WITH QUADRATIC BOUND

In Ref. [22] based on extensive numerical simulation a quadratic bound (lower bound) was proposed for a scaled cumulant generating function for a multiaffinity time-homogeneous discrete state continuous-time Markov process in steady state. Later on, in Ref. [20], a rigorous proof for the quadratic bound was given for systems following continuous-time Markov jump processes in steady state. For our single-affinity problem and transient dynamics, the quadratic bound (QB) in terms of the CGF translates to

$$\mathcal{G}^{\text{QB}}(u) = \langle Q \rangle \left[u + \frac{u^2 \langle Q \rangle}{\langle \Sigma \rangle} \right], \quad (D1)$$

where u is treated as a real variable (the CGFs obtained in the main text should be analytically continued, $iu \rightarrow u$).

Once any CGF satisfies the above quadratic bound one can immediately prove the T-TUR in Eq. (1). Since we have the exact expressions for the CGFs for three exactly solvable model systems, we compare numerically the CGFs with the quadratic bound in Eq. (D1). We found that, for the harmonic oscillator problem since T-TUR is always valid, the above quadratic bound is always respected as shown in Fig. 7 for two different values of the TUR ratio. In contrast, for the two-qubit and the hybrid spin-oscillator model we observe that whenever the T-TUR is valid the above quadratic bound is respected [Figs. 8(a) and 9(a)] and, expectedly, the violation of the quadratic bound is observed whenever the T-TUR ratio is smaller than 2, as shown in Figs. 8(b) and 9(b).

- [1] F. Ritort, Nonequilibrium fluctuations in small systems: From physics to biology, *Adv. Chem. Phys.* **137**, 31 (2008).
 [2] J. P. S. Peterson, T. B. Batalhão, M. Herrera, A. M. Souza, R. S. Sarthour, I. S. Oliveira, and R. M. Serra, Experimental Characterization of a Spin Quantum Heat Engine, *Phys. Rev. Lett.* **123**, 240601 (2019).

- [3] S. Rahav, U. Harbola, and S. Mukamel, Heat fluctuations and coherences in a quantum heat engine, *Phys. Rev. A* **86**, 043843 (2012).
 [4] D. J. Evans, E. G. D. Cohen, and G. P. Morriss, Probability of Second Law Violations in Shearing Steady States, *Phys. Rev. Lett.* **71**, 2401 (1993).

- [5] G. Gallavotti and E. G. D. Cohen, Dynamical Ensembles in Nonequilibrium Statistical Mechanics, *Phys. Rev. Lett.* **74**, 2694 (1995).
- [6] C. Jarzynski, Nonequilibrium Equality for Free Energy Differences, *Phys. Rev. Lett.* **78**, 2690 (1997).
- [7] J. Kurchan, Fluctuation theorem for stochastic dynamics, *J. Phys. A: Math. Gen.* **31**, 3719 (1998).
- [8] J. L. Lebowitz and H. Spohn, A Gallavotti-Cohen-type symmetry in the large deviation functional for stochastic dynamics, *J. Stat. Phys.* **95**, 333 (1999).
- [9] C. Jarzynski and D. K. Wójcik, Classical and Quantum Fluctuation Theorems for Heat Exchange, *Phys. Rev. Lett.* **92**, 230602 (2004).
- [10] M. Esposito, U. Harbola, and S. Mukamel, Nonequilibrium fluctuations, fluctuation theorems, and counting statistics in quantum systems, *Rev. Mod. Phys.* **81**, 1665 (2009).
- [11] M. Campisi, P. Hänggi, and P. Talkner, Colloquium: Quantum fluctuation relations: Foundations and applications, *Rev. Mod. Phys.* **83**, 771 (2011).
- [12] C. Jarzynski, Equalities and inequalities: Irreversibility and the second law of thermodynamics at the nanoscale, *Annu. Rev. Condens. Matter Phys.* **2**, 329 (2011).
- [13] K. Saito and Y. Utsumi, Symmetry in full counting statistics, fluctuation theorem, and relations among nonlinear transport coefficients in the presence of a magnetic field, *Phys. Rev. B* **78**, 115429 (2008).
- [14] M. Campisi, P. Talkner, and P. Hänggi, Influence of measurements on the statistics of work performed on a quantum system, *Phys. Rev. E* **83**, 041114 (2011).
- [15] U. Seifert, Stochastic thermodynamics, fluctuation theorems, and molecular machines, *Rep. Prog. Phys.* **75**, 126001 (2012).
- [16] U. Seifert, Stochastic thermodynamics: Principles and perspective, *Eur. Phys. J. B* **64**, 423 (2008).
- [17] R. Kosloff, Quantum thermodynamics and open-systems modeling, *J. Chem. Phys.* **150**, 204105 (2019).
- [18] S. Vinjanampathy and J. Anders, Quantum thermodynamics, *Contemp. Phys.* **57**, 545 (2016).
- [19] A. C. Barato and U. Seifert, Thermodynamic Uncertainty Relation for Biomolecular Processes, *Phys. Rev. Lett.* **114**, 158101 (2015).
- [20] T. R. Gingrich, J. M. Horowitz, N. Perunov, and J. L. England, Dissipation Bounds All Steady State Current Fluctuations, *Phys. Rev. Lett.* **116**, 120601 (2016).
- [21] M. Poletini, A. Lazarescu, and M. Esposito, Tightening the uncertainty principle for stochastic currents, *Phys. Rev. E* **94**, 052104 (2016).
- [22] P. Pietzonka, A. C. Barato, and U. Seifert, Universal bounds on current fluctuations, *Phys. Rev. E* **93**, 052145 (2016).
- [23] C. Hyeon and W. Hwang, Physical insight into the thermodynamic uncertainty relation using Brownian motion in tilted periodic potentials, *Phys. Rev. E* **96**, 012156 (2017).
- [24] J. M. Horowitz and T. R. Gingrich, Proof of the finite-time thermodynamic uncertainty relation for steady-state currents, *Phys. Rev. E* **96**, 020103(R) (2017).
- [25] S. Pigolotti, I. Neri, E. Roldán, and F. Jülicher, Generic Properties of Stochastic Entropy Production, *Phys. Rev. Lett.* **119**, 140604 (2017).
- [26] K. Proesmans and C. V. den Broeck, Discrete-time thermodynamic uncertainty relation, *Europhys. Lett.* **119**, 20001 (2017).
- [27] W. Hwang, and C. Hyeon, Energetic costs, precision, and transport efficiency of molecular motors, *J. Phys. Chem. Lett.* **9**, 513 (2018).
- [28] R. Marsland III, W. Cui, and J. M. Horowitz, The thermodynamic uncertainty relation in biochemical oscillations, *J. R. Soc. Interface* **16**, 20190098 (2019).
- [29] S. Lee, C. Hyeon, and J. Jo, Thermodynamic uncertainty relation of interacting oscillators in synchrony, *Phys. Rev. E* **98**, 032119 (2018).
- [30] M. Shreshtha and R. J. Harris, Thermodynamic uncertainty for run-and-tumble-type processes, *Europhys. Lett.* **126**, 40007 (2019).
- [31] J. P. Garrahan, Simple bounds on fluctuations and uncertainty relations for first-passage times of counting observables, *Phys. Rev. E* **95**, 032134 (2017).
- [32] T. R. Gingrich and J. M. Horowitz, Fundamental Bounds on First Passage Time Fluctuations for Currents, *Phys. Rev. Lett.* **119**, 170601 (2017).
- [33] A. Dechant, Multidimensional thermodynamic uncertainty relations, *J. Phys. A: Math. Theor.* **52**, 035001 (2019).
- [34] P. Pietzonka, F. Ritort, and U. Seifert, Finite-time generalization of the thermodynamic uncertainty relation, *Phys. Rev. E* **96**, 012101 (2017).
- [35] G. Falasco, M. Esposito, and J.-C. Delvenne, Unifying thermodynamic uncertainty relations, *New J. Phys.* **22**, 053046 (2020).
- [36] P. P. Potts and P. Samuelsson, Thermodynamic uncertainty relations including measurement and feedback, *Phys. Rev. E* **100**, 052137 (2019).
- [37] T. Koyuk, U. Seifert, and P. Pietzonka, A generalization of the thermodynamic uncertainty relation to periodically driven systems, *J. Phys. A: Math. Theor.* **52**, 02LT02 (2018).
- [38] K. Macieszczak, K. Brandner, and J. P. Garrahan, Unified Thermodynamic Uncertainty Relations in Linear Response, *Phys. Rev. Lett.* **121**, 130601 (2018).
- [39] T. Van Vu and Y. Hasegawa, Uncertainty relation under information measurement and feedback control, *J. Phys. A: Math. Theor.* **53**, 075001 (2020).
- [40] K. Proesmans and J. M. Horowitz, Hysteretic thermodynamic uncertainty relation for systems with broken time-reversal symmetry, *J. Stat. Mech.* (2019) 054005.
- [41] A. C. Barato, R. Chetrite, A. Faggionato, and D. Gabrielli, Bounds on current fluctuations in periodically driven systems, *New J. Phys.* **20**, 103023 (2018).
- [42] Y. Hasegawa and T. Van Vu, Fluctuation Theorem Uncertainty Relation, *Phys. Rev. Lett.* **123**, 110602 (2019).
- [43] Y. Hasegawa and T. V. Vu, Uncertainty relations in stochastic processes: An information inequality approach, *Phys. Rev. E* **99**, 062126 (2019).
- [44] M. L. Rosinberg and G. Tarjus, Comment on Thermodynamic uncertainty relation for time-delayed Langevin systems, [arXiv:1810.12467](https://arxiv.org/abs/1810.12467).
- [45] T. R. Gingrich, G. M. Rotskoff, and J. M. Horowitz, Inferring dissipation from current fluctuations, *J. Phys. A: Math. Theor.* **50**, 184004 (2017).
- [46] A. Dechant and S.-i. Sasa, Current fluctuations and transport efficiency for general Langevin systems, *J. Stat. Mech.* (2018) 063209.
- [47] I. Di Terlizzi and M. Baiesi, Kinetic uncertainty relation, *J. Phys. A: Math. Theor.* **52**, 02LT03 (2018).

- [48] K. Brandner, T. Hanazato, and K. Saito, Thermodynamic Bounds on Precision in Ballistic Multiterminal Transport, *Phys. Rev. Lett.* **120**, 090601 (2018).
- [49] D. Gupta and A. Maritan, Thermodynamic uncertainty relations via second law of thermodynamics, *Eur. Phys. J. B* **93**, 28 (2020).
- [50] H.-M. Chun, L. P. Fischer, and U. Seifert, Effect of a magnetic field on the thermodynamic uncertainty relation, *Phys. Rev. E* **99**, 042128 (2019).
- [51] K. Ptasiński, Coherence-enhanced constancy of a quantum thermoelectric generator, *Phys. Rev. B* **98**, 085425 (2018).
- [52] B. K. Agarwalla and D. Segal, Assessing the validity of the thermodynamic uncertainty relation in quantum systems, *Phys. Rev. B* **98**, 155438 (2018).
- [53] S. Saryal, H. Friedman, D. Segal, and B. K. Agarwalla, Thermodynamic uncertainty relation in thermal transport, *Phys. Rev. E* **100**, 042101 (2019).
- [54] J. Liu and D. Segal, Thermodynamic uncertainty relation in quantum thermoelectric junctions, *Phys. Rev. E* **99**, 062141 (2019).
- [55] S. Kheradsoud, N. Dashti, M. Misiorny, P. P. Potts, J. Splettstoesser, and P. Samuelsson, Power, efficiency and fluctuations in a quantum point contact as steady-state thermoelectric heat engine, *Entropy* **21**, 777 (2019).
- [56] A. M. Timpanaro, G. Guarnieri, J. Goold, and G. T. Landi, Thermodynamic Uncertainty Relations from Exchange Fluctuation Theorems, *Phys. Rev. Lett.* **123**, 090604 (2019).
- [57] H. Vroylandt, K. Proesmans, and T. R. Gingrich, Isometric uncertainty relations, *J. Stat. Phys.* **178**, 1039 (2020).
- [58] G. Guarnieri, G. T. Landi, S. R. Clark, and J. Goold, Thermodynamics of precision in quantum non-equilibrium steady states, *Phys. Rev. Research* **1**, 033021 (2019).
- [59] J. M. Horowitz and T. R. Gingrich, Thermodynamic uncertainty relations constrain non-equilibrium fluctuations, *Nat. Phys.* **16**, 15 (2020).
- [60] T. Koyuk and U. Seifert, Thermodynamic Uncertainty Relation for Time-Dependent Driving, *Phys. Rev. Lett.* **125**, 260604 (2020).
- [61] Y. Hasegawa, Thermodynamic Uncertainty Relation for Open Quantum Systems, *Phys. Rev. Lett.* **126**, 010602 (2021).
- [62] M. F. Sacchi, Thermodynamic uncertainty relations for bosonic Otto engines, *Phys. Rev. E* **103**, 012111 (2021).
- [63] M. W. Jack, N. J. López-Alamilla, and K. J. Challis, Thermodynamic uncertainty relations and molecular-scale energy conversion, *Phys. Rev. E* **101**, 062123 (2020).
- [64] H. Tajima and K. Funo, Superconducting-like heat current: Effective cancellation of current-dissipation trade off by quantum coherence, [arXiv:2004.13412](https://arxiv.org/abs/2004.13412).
- [65] S. Rana and A. C. Barato, Precision and dissipation of a stochastic Turing pattern, *Phys. Rev. E* **102**, 032135 (2020).
- [66] D. M. Busiello and S. Pigolotti, Hyperaccurate currents in stochastic thermodynamics, *Phys. Rev. E* **100**, 060102(R) (2019).
- [67] Y. Hasegawa, Quantum Thermodynamic Uncertainty Relation for Continuous Measurement, *Phys. Rev. Lett.* **125**, 050601 (2020).
- [68] H. M. Friedman, B. K. Agarwalla, O. Shein-Lumbroso, O. Tal, and D. Segal, Thermodynamic uncertainty relation in atomic-scale quantum conductors, *Phys. Rev. B* **101**, 195423 (2020).
- [69] S. Pal, S. Saryal, D. Segal, T. S. Mahesh, and B. K. Agarwalla, Experimental study of the thermodynamic uncertainty relation, *Phys. Rev. Research* **2**, 022044(R) (2020).
- [70] W. D. Pineros and T. Tlusty, Kinetic proofreading and the limits of thermodynamic uncertainty, *Phys. Rev. E* **101**, 022415 (2020).
- [71] G. Paneru, S. Dutta, T. Tlusty, and H. K. Pak, Approaching and violating thermodynamic uncertainty bounds in measurements of fluctuation-dissipation tradeoffs of information engines, *Phys. Rev. E* **102**, 032126 (2020).
- [72] S. K. Manikandan, D. Gupta, and S. Krishnamurthy, Inferring Entropy Production from Short Experiments, *Phys. Rev. Lett.* **124**, 120603 (2020).
- [73] B. K. Agarwalla, H. Li, B. Li, and J.-S. Wang, Exchange fluctuation theorem for heat transport between multiterminal harmonic systems, *Phys. Rev. E* **89**, 052101 (2014).
- [74] B. K. Agarwalla, B. Li, and J.-S. Wang, Full-counting statistics of heat transport in harmonic junctions: Transient, steady states, and fluctuation theorems, *Phys. Rev. E* **85**, 051142 (2012).
- [75] K. Saito and A. Dhar, Fluctuation Theorem in Quantum Heat Conduction, *Phys. Rev. Lett.* **99**, 180601 (2007).
- [76] T. Denzler and E. Lutz, Heat distribution of a quantum harmonic oscillator, *Phys. Rev. E* **98**, 052106 (2018).
- [77] G. T. Landi and D. Karevski, Fluctuations of the heat exchanged between two quantum spin chains, *Phys. Rev. E* **93**, 032122 (2016).
- [78] J. Schwinger, Brownian motion of a quantum oscillator, *J. Math. Phys.* **2**, 407 (1961).
- [79] L. V. Keldysh, Diagram technique for nonequilibrium processes, *J. Expt. Theor. Phys. (U.S.S.R.)* **47**, 1515 (1964) [*Sov. Phys. JETP* **20**, 1018 (1965)].
- [80] J. Rammer and H. Smith, Quantum field-theoretical methods in transport theory of metals, *Rev. Mod. Phys.* **58**, 323 (1986).
- [81] G. D. Mahan, *Many-Particle Physics*, 3rd ed. (Kluwer Academic, New York, 2000).
- [82] H. Haug and A.-P. Jauho, *Quantum Kinetics in Transport and Optics of Semiconductors*, 2nd ed. (Springer, New York, 2008).
- [83] S. Akagawa and N. Hatano, The exchange fluctuation theorem in quantum mechanics, *Prog. Theor. Phys.* **121**, 1157 (2009).
- [84] L. Mazzola, G. De Chiara, and M. Paternostro, Measuring the Characteristic Function of the Work Distribution, *Phys. Rev. Lett.* **110**, 230602 (2013).
- [85] R. Dornier, S. R. Clark, L. Heaney, R. Fazio, J. Goold, and V. Vedral, Extracting Quantum Work Statistics and Fluctuation Theorems by Single-Qubit Interferometry, *Phys. Rev. Lett.* **110**, 230601 (2013).
- [86] M. Campisi, R. Blattmann, S. Kohler, D. Zueco, and P. Hanggi, Employing circuit QED to measure non-equilibrium work fluctuations, *New J. Phys.* **15**, 105028 (2013).
- [87] S. Pal, T. S. Mahesh, and B. K. Agarwalla, Experimental demonstration of the validity of the quantum heat-exchange fluctuation relation in an NMR setup, *Phys. Rev. A* **100**, 042119 (2019).
- [88] C. Gerry and P. Knight, *Introductory Quantum Optics* (Cambridge University Press, Cambridge, UK, 2005).